



Executive summary

Joint particle filtering of multiple maneuvering targets from unassociated measurements

Problem area

This report considers the problem of maneuvering target tracking from possibly missing and false measurements with non-homogeneous density of false measurements. For this problem particle filtering is studied as an alternative for multitarget track maintenance versions of Interacting Multiple Model (IMM) in combination with Probabilistic Data Association (PDA) or Joint PDA (JPDA)

Description of work

The approach taken is to first characterize the problem in terms of filtering for a jump linear descriptor system with both Markovian and i.i.d. coefficients, and next to use this for the derivation of the exact recursive equation for the Bayesian filter. This result is used to develop two Sampling Importance Resampling (SIR) type particle filters, one which resamples a fixed number of joint particles (SIR joint particle filter) and one which resamples a fixed number of joint particles per joint mode (SIR-H joint particle filter). It is also shown that application of some approximating assumptions to the exact Bayesian filter equations leads to a compact version of the Interacting Multiple Model Joint

probabilistic Data Association (IMMJPDA) filter. For this (compact) IMMJPDA filter also a track-coalescence-avoiding version (IMMJPDA*) is developed by introduction of a particular pruning of permutation hypotheses. All four novel filter algorithms cover the situation of non-homogeneous density of false measurements.

Results and conclusions

Through Monte Carlo simulations for a series of simple scenarios with two targets and two associated tracks these four novel filters have been compared to each other and to a filter which runs per track a single target IMMJPDA. All four clearly outperformed IMMJPDA. The SIR-H joint particle filter appears to approximate the Bayesian filter well, whereas the SIR joint particle filter did not. On all scenarios, IMMJPDA* performs significantly better than IMMJPDA and sometimes even remarkably close to the performance of the SIR-H joint particle filter.

Applicability

The applicability of the work comprises the implementation of the resulting filtering algorithms in a multitarget tracker, in particular the Advanced surveillance Tracker And Server ARTAS.

Report no.

NLR-TP-2006-692

Author(s)

H.A.P. Blom, E.A. Bloem

Report classification

Unclassified

Date

September 2006

Knowledge area(s)

Advanced (sensor-) information processing

Descriptor(s)

Bayesian filtering
Multitarget tracking
Sudden maneuvers
False measurements
Missing measurements
Descriptor system
Particle filtering



NLR-TP-2006-692

Joint particle filtering of multiple maneuvering targets from unassociated measurements

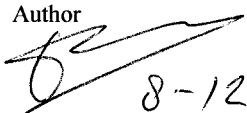
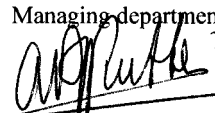
H.A.P. Blom and E.A. Bloem

This report contains a publication in Journal of Advancement Information Fusion, July 2006.

This report may be cited on condition that full credit is given to NLR and the authors.

Customer: National Aerospace Laboratory NLR
Working Plan number: 2005 AT.1.C
Owner: National Aerospace Laboratory NLR
Division: Air Transport
Distribution: Unlimited
Classification title: Unclassified
September 2006

Approved by:

Author  8-12-06	Reviewer Anonymous peer reviewers	Managing department  22/12/06
--	--------------------------------------	--

Joint particle filtering of multiple maneuvering targets from unassociated measurements

Henk A.P. Blom and Edwin A. Bloem
National Aerospace Laboratory NLR
Amsterdam, The Netherlands
e-mail: blom@nlr.nl, bloem@nlr.nl

Abstract—The problem of maintaining tracks of multiple maneuvering targets from unassociated measurements is formulated as a problem of estimating the hybrid state of a Markov jump linear system from measurements made by a descriptor system with independent, identically distributed (i.i.d.) stochastic coefficients. This characterization is exploited to derive the exact equation for the Bayesian recursive filter, to develop two novel Sampling Importance Resampling (SIR) type particle filters, and to derive approximate Bayesian filters which use for each target one Gaussian per maneuver mode. The two approximate Bayesian filters are a compact and a track-coalescence avoiding version of Interacting Multiple Model Joint Probabilistic Data Association (IMMJPDA). The relation of each of the four novel filter algorithms with literature is well explained. Through Monte Carlo simulations for a two target example, these four filters are compared to each other and to the approach of using one IMPDA filter per target track. The Monte Carlo simulation results show that each of the four novel filters clearly outperforms the IMPDA approach. The results also show under which conditions the IMMJPDA type filters perform close to exact Bayesian filtering, and under which conditions not.

Index Terms—Bayesian filtering, Multitarget tracking, Sudden maneuvers, false measurements, Missing measurements, Descriptor system, particle filtering.

1. INTRODUCTION

In literature approximate Bayesian approaches towards maintaining tracks of multiple maneuvering targets from unassociated measurements have focussed on the development of combinations of Interacting Multiple Model (IMM) and Joint Probabilistic Data Association (JPDA) approaches. Initially, combinations of IMM and JPDA have been developed along two heuristic directions. Bar-Shalom et al. [4] heuristically developed an IMMJPDA-Coupled filter for situations where the measurements of two targets are unresolved during periods of close encounter. The filters of the individual targets are coupled through cross-target-covariance terms. The filtering results obtained have not been very encouraging to continue this heuristic approach. De Feo et al. [20] combined JPDA and a rather crude approximation of IMM, under the name IMMJPDA. The first proper combination of IMM and JPDA has been developed by Chen & Tugnait [18]. Focus of this development was on showing that fixed-lag IMMJPDA smoothing performed far better than IMMJPDA filtering at the cost of 3 scans delay. In [9], [10] we used the descriptor

system approach [8] to develop a track-coalescence-avoiding version of IMMJPDA (for short IMMJPDA*). Moreover, we showed that both IMMJPDA and IMMJPDA* perform much better than just applying IMPDA filtering per maintained track. In spite of these developments it remains unclear how IMMJPDA and IMMJPDA* filtering performs in comparison with the exact Bayesian filter.

This motivates to study the Sampling Importance Resampling (SIR) based Particle Filter (PF) paradigm [21], [28], [43] for maintaining tracks of multiple maneuvering targets from unassociated measurements. During the last decade this paradigm has been recognized as a practical means in approximating an exact Bayesian filter arbitrarily well. This has stimulated the development of a large variety of particle filters (e.g. [1], [22], [38], [42]) that typically outperform established approximate non-linear filtering and target track maintenance approaches such as Extended Kalman Filtering, Probabilistic Data Association (PDA), Interacting Multiple Model (IMM) algorithm, and their combinations.

The extension of these results to multiple target tracking situations also received significant attention. Early on it was recognized that the JPDA formalism provided a logical starting point for this development. Gordon [26] developed a SIR-PF version by replacing JPDA's Gaussian density by a density the evolution of which is approximated with help of a SIR particle filter. Avitzour [2] developed a more advanced SIR particle filter by using joint-target particles; we refer to this as SIR joint PF. Karlsson and Gustafsson [30] compared the RMS position errors of a SIR joint PF with those of a JPDA filter for maintaining tracks in an example of two perpendicular crossing targets. For this "easy" example the difference in performance appeared to be small. Salmond et al. [45] showed that a SIR joint PF works well for the initialization of two non-maneuvring targets that start from the same initial position. Gordon et al. [27] developed a SIR joint PF approach for tracking a group of targets, the members of which stay close to each other. Through several complementary studies, efficiency improvements have been developed for these particle filters, e.g. [29], [41], [42], [48]. To track multiple objects for robotic vision, Schultz et al. [46] developed an occlusion extension for SIR PF and showed that this outperformed JPDA on a multi person tracking problem. Tracking multiple objects with occlusion situations by SIR joint PF for robotic vision has been shown by [33] and [34].

A complementary development in SIR particle filtering is to use sensor measurements at pixel level as observations.

⁰Manuscript received July 7, 2004; revised December 31, 2005 and May 2, 2006; released for publication May 15, 2006. Refereeing of this contribution was handled by Shozo Mori.

This allows handling the problems of target detection and target tracking in an integrated way, and thus to shortcut the traditional sequence of signal processing first, followed by target detection (thresholding) and then target tracking. The feasibility of a track-before-detect particle filtering approach has been introduced in [15], [44] for a single target. Extensions to multiple targets have been developed in [40] using single target particles, and in [17], [32], [35] using joint particles. For the current paper we assume that track maintenance has to be performed on the basis of detected measurement observations, and that pixel level sensor measurements are not available. Hence, the track-before-detect problem setting goes beyond the scope of the current study.

The aim of this paper is to extend the SIR joint particle filter approach towards track maintenance, to the situation of multiple manoeuvring targets and to evaluate for an example how the performance of these particle filters compares with IMMJPDA and IMMJPDA* filtering. This asks for the combination of SIR joint PF for unassociated measurements with SIR PF for tracking a suddenly manoeuvring target [16], [36], [37]. The basis for this integration is provided by the exact Bayesian filter for this particular problem. We developed such an exact Bayesian characterisation using the descriptor system approach [10], [14]. The current paper extends these results in the sense of incorporating a non-homogeneous false measurement density [39].

The specialty of this exact characterization is that both the mode switching and the data association are performed jointly for all targets and that false plot density is non-homogeneous. Based on such exact equations, we develop a standard SIR particle filter to evaluate the exact Bayesian equations. A weakness of this standard SIR joint particle filter is that after a resampling step for some of the joint modes there may be hardly any or even no particles left. In theory this can be compensated by significantly increasing the number of particles. However, a more effective approach is to resample a fixed number of joint particles per joint mode. We refer to this as hybrid SIR joint particle filtering. Through Monte Carlo simulations for a simple example the standard SIR and hybrid SIR joint particle filters are compared with the following three combinations of IMM and PDA:

- IMM-PDA filter, which updates an individual IMM track using MMPDA [25] and implicitly assuming there are no other targets;
- A compact version of IMMJPDA, which we derive in this paper in a systematic way from the exact Bayesian filter equations; and
- The track coalescence avoiding version (IMMJPDA*) of this compact IMMJPDA.

The paper is organized as follows. Section II formulates the multi target track maintenance problem considered. Section III embeds this in filtering for a jump linear descriptor system. Section IV develops an exact Bayesian characterization of the evolution of the conditional density for the state of the multiple targets. Section V develops the standard SIR joint particle filter. Section VI develops the hybrid SIR joint particle filter. Section VII adopts the IMMJPDA assumptions, and shows

the impact on the filter equations relative to those of [18]. Section VIII develops IMMJPDA*. Section IX illustrates and compares the performance of these filters through Monte Carlo simulation results. As a performance reference we also run single target IMM-PDA filters on the same scenario. Finally, Section X draws conclusions.

2. MULTITARGET TRACK MAINTENANCE PROBLEM

Consider M targets and assume that the state of the i -th target is modelled as a jump linear system:

$$x_t^i = a^i(\theta_t^i)x_{t-1}^i + b^i(\theta_t^i)w_t^i, \quad i = 1, \dots, M, \quad (1)$$

where x_t^i is the n -vectorial state of the i -th target, θ_t^i is the Markovian switching mode of the i -th target and assumes values from $\mathbb{M} = \{1, \dots, N\}$ according to a transition probability matrix Π^i , $a^i(\theta_t^i)$ and $b^i(\theta_t^i)$ are $(n \times n)$ - and $(n \times n')$ -matrices and w_t^i is a sequence of i.i.d. standard Gaussian variables of dimension n' with w_t^i , w_t^j independent for all $i \neq j$ and $w_t^i, (x_0^i, \theta_0^i)$, (x_0^j, θ_0^j) independent for all $i \neq j$. At $t = 0$, the joint density $p_{x_0^i, \theta_0^i}$ is known for each $i \in [1, M]$; typically these are i -variant.

A set of measurements consists of measurements originating from targets and measurements originating from clutter. We assume that a potential measurement originating from target i is also modelled as a jump linear system:

$$z_t^i = h^i(\theta_t^i)x_t^i + g^i(\theta_t^i)v_t^i, \quad i = 1, \dots, M \quad (2)$$

where z_t^i is an m -vector, $h^i(\theta_t^i)$ is an $(m \times n)$ -matrix and $g^i(\theta_t^i)$ is an $(m \times m')$ -matrix, and v_t^i is a sequence of i.i.d. standard Gaussian variables of dimension m' with v_t^i and v_t^j independent for all $i \neq j$. Moreover v_t^i is independent of x_0^j and w_t^j for all i, j .

Let $x_t \triangleq \text{Col}\{x_t^1, \dots, x_t^M\}$, $\theta_t \triangleq \text{Col}\{\theta_t^1, \dots, \theta_t^M\}$, $A(\theta_t) \triangleq \text{Diag}\{a^1(\theta_t^1), \dots, a^M(\theta_t^M)\}$, $B(\theta_t) \triangleq \text{Diag}\{b^1(\theta_t^1), \dots, b^M(\theta_t^M)\}$, and $w_t \triangleq \text{Col}\{w_t^1, \dots, w_t^M\}$. Then we can model the state of our M targets as follows:

$$x_t = A(\theta_t)x_{t-1} + B(\theta_t)w_t \quad (3)$$

with A and B of size $Mn \times Mn$ and $Mn \times Mn'$ respectively, with $\{\theta_t\}$ assuming values from \mathbb{M}^M according to transition probability matrix $\Pi = [\Pi_{\eta, \theta}]$. If the M targets switch mode independently of each other, then:

$$\Pi_{\eta, \theta} = \prod_{i=1}^M \Pi_{\eta^i, \theta^i} \quad (4)$$

for every $\eta \in \mathbb{M}^M$ and $\theta \in \mathbb{M}^M$.

Next with $z_t \triangleq \text{Col}\{z_t^1, \dots, z_t^M\}$, $H(\theta_t) \triangleq \text{Diag}\{h^1(\theta_t^1), \dots, h^M(\theta_t^M)\}$, $G(\theta_t) \triangleq \text{Diag}\{g^1(\theta_t^1), \dots, g^M(\theta_t^M)\}$, and $v_t \triangleq \text{Col}\{v_t^1, \dots, v_t^M\}$, we obtain:

$$z_t = H(\theta_t)x_t + G(\theta_t)v_t \quad (5)$$

with H and G of size $Mm \times Mn$ and $Mm \times Mm'$ respectively.

We next assume that with a non-zero detection probability,

P_d^i , target i is indeed observed at moment t . In addition to this there may be false measurements, the density of which is not homogeneous. Similar as [39] we assume that the number of false measurements at moment t , F_t , has a Poisson distribution:

$$p_{F_t}(F) = \frac{(\hat{F}_t)^F}{F!} \exp(-\hat{F}_t), \quad F = 0, 1, 2, \dots \quad (6.a)$$

$$= 0, \quad \text{else}$$

where \hat{F}_t is the expected number of false measurements. Let f_t denote the column vector of i.i.d. false measurements, then the conditional density of f_t given F_t satisfies:

$$p_{f_t|F_t}(f|F) = \prod_{i=1}^F p_f(f^i) \quad (6.b)$$

where $p_f(\cdot)$ is the (measurable) probability density function of a false measurement. Hence, the local density $\lambda(\cdot)$ of false measurements satisfies:

$$\lambda(f^i) = \hat{F}_t p_f(f^i) \quad (6.c)$$

Furthermore we assume that the process $\{F_t, f_t\}$ is a sequence of independent vectors, which are independent of $\{x_t\}$, $\{w_t\}$ and $\{v_t\}$.

At moment $t = 1, 2, \dots, T$ a vector observation y_t is made, the components of which consist of the potential observations z_t^i of the detected targets plus the false measurements $\{F_t, f_t\}$. The multi-target track maintenance problem considered is to estimate x_t, θ_t given observations $Y_t \triangleq \{y_s; 0 \leq s \leq t\}$ with y_0 representing the initial joint density p_{x_0, θ_0} .

3. STOCHASTIC MODELLING OF OBSERVATION EQUATION

This section characterizes the exact relation between observation vector y_t and the false and potential observations at moment $t > 0$. For this we largely follow [8]. The measurement vector y_t consists of measurements originating from targets and measurements originating from clutter. Firstly the relation for measurements originating from targets is identified. Subsequently the clutter measurements are randomly inserted between the target measurements.

Let $\phi_{i,t} \in \{0,1\}$ be the detection indicator for target i , which assumes the value one with a time invariant probability $P_d^i > 0$, independently of $\phi_{j,t}$, $j \neq i$ and independently of the processes introduced in section II. This approach yields the following detection indicator vector ϕ_t of size M :

$$\phi_t \triangleq \text{Col}\{\phi_{1,t}, \dots, \phi_{M,t}\}.$$

Thus, the number of detected targets is $D_t \triangleq \sum_{i=1}^M \phi_{i,t}$. Furthermore, we assume that $\{\phi_t\}$ is a sequence of i.i.d. vectors.

In order to link the detection indicator vector with the measurement model, we introduce the following operator Φ : for an arbitrary vector ϕ' of length M' and having $(0,1)$ valued components, we define $D(\phi') \triangleq \sum_{i=1}^{M'} \phi'_i$ and the operator Φ producing $\Phi(\phi')$ as a $(0,1)$ -valued matrix of size $D(\phi') \times M'$ of which the i th row equals the i th non-zero row of $\text{Diag}\{\phi'\}$.

Next we define, for $D_t > 0$, a vector that contains all measurements originating from targets in a fixed order.

$$\tilde{z}_t \triangleq \underline{\Phi}(\phi_t) z_t, \quad \text{where} \quad \underline{\Phi}(\phi_t) \triangleq \Phi(\phi_t) \otimes I_m,$$

with I_m a unit-matrix of size m , and \otimes the Kronecker product, i.e.

$$\begin{bmatrix} a & b \\ c & d \end{bmatrix} \otimes I_m \triangleq \begin{bmatrix} aI_m & \vdots & bI_m \\ \vdots & \ddots & \vdots \\ cI_m & \vdots & dI_m \end{bmatrix}$$

In reality, however, we do not know in which order the targets are observed. Hence, we introduce the stochastic $D_t \times D_t$ permutation matrix χ_t , which is independent of the processes introduced in section II and is conditionally independent of $\{\phi_t\}$ given D_t . We also assume that $\{\chi_t\}$ is a sequence of independent matrices. Hence, for $D_t > 0$,

$$\tilde{\tilde{z}}_t \triangleq \underline{\chi}_t \tilde{z}_t, \quad \text{where} \quad \underline{\chi}_t \triangleq \chi_t \otimes I_m,$$

is a vector that contains all measurements originating from targets at moment t in a random order.

Let the random variable L_t be the total number of measurements at moment t . Thus,

$$L_t = D_t + F_t$$

We next describe the relation between the potential measurement vector z_t , the false plot vector f_t and the measurement vector $y_t \triangleq \text{Col}\{y_{1,t}, \dots, y_{L_t,t}\}$, where $y_{i,t}$ denotes the i -th m -vectorial measurement at moment t . Because y_t contains a random mixture of D_t target measurements and $L_t - D_t$ false measurements, the relation between z_t and y_t can be characterized by the following pair of equations for the target and false measurements respectively:

$$\begin{aligned} \underline{\Phi}(\psi_t) y_t &= \underline{\chi}_t \underline{\Phi}(\phi_t) z_t, & \text{if } D_t > 0, \\ &= \{\}, & \text{if } D_t = 0 \end{aligned} \quad (7.a)$$

$$\begin{aligned} \underline{\Phi}(\psi_t^*) y_t &= f_t, & \text{if } L_t > D_t, \\ &= \{\}, & \text{if } L_t = D_t \end{aligned} \quad (7.b)$$

where ψ_t, ψ_t^*, χ_t are explained below.

First we explain the target measurement eq. (7.a). This equation has stochastic i.i.d. coefficients $\underline{\Phi}(\psi_t)$ and $\underline{\chi}_t \underline{\Phi}(\phi_t)$. The detected target measurements in the observation vector y_t are in random order. Hence the potential detected measurements of targets need to be randomly mixed. To perform this by a simple matrix multiplication, a sequence of independent stochastic permutation matrices $\{\chi_t\}$ of size $D_t \times D_t$ is defined and assumed to be independent of $\{\phi_t\}$. To take into account the measurement vector size m , χ_t needs to be "inflated" to the proper size of $D_t m$ by means of the Kronecker product with I_m . To this end, $\underline{\chi}_t \triangleq \chi_t \otimes I_m$ with I_m a unit-matrix of size m , and \otimes the Kronecker product. Hence $\underline{\chi}_t \underline{\Phi}(\phi_t) z_t$ is a column vector of potential detected measurements of targets in random order.

$\psi_t \triangleq \text{Col}\{\psi_{1,t}, \dots, \psi_{L_t,t}\}$ is the target indicator vector, where $\psi_{i,t} \in \{0,1\}$ is a target indicator at moment t for measurement i , which assumes the value one if measurement i belongs to

a detected target and zero if measurement i is false. Because there are as many detected targets as target measurements, the following constraint applies:

$$D(\psi_t) = D(\phi_t) \quad (8)$$

Under this equality constraint, $\{\psi_t\}$ is a sequence of independent vectors that is D_t -conditionally independent of all earlier defined processes.

In order to let ψ_t select the correct measurements by simple matrix multiplication, the matrix operator Φ defined above is used. To take into account the measurement vector size m , $\Phi(\psi_t)$ needs to be "inflated" to the proper size of $D_t m$ by means of the Kronecker product with I_m . To this end, $\underline{\Phi}(\psi') \triangleq \Phi(\psi') \otimes I_m$ with I_m a unit-matrix of size m , and \otimes the Kronecker product. Hence $\underline{\Phi}(\psi_t)y_t$ is a column vector that contains all detected target measurements in y_t .

$\psi_t^* \triangleq \text{Col}\{\psi_{1,t}^*, \dots, \psi_{L_t,t}^*\}$ is a false indicator vector of size L_t with $\psi_{i,t}^* = 1 - \psi_{i,t}$. To select the false measurements by matrix multiplication, the matrix operator Φ is used again. Hence $\underline{\Phi}(\psi_t^*)y_t$ is a column vector that contains all false measurements from y_t .

Finally we develop a characterization for y_t . For this we first verify the following for $L_t > D_t > 0$:

$$\Phi(\psi_t)^T \Phi(\psi_t) + \Phi(\psi_t^*)^T \Phi(\psi_t^*) = I_{L_t \times L_t}$$

Hence

$$y_t = [\Phi(\psi_t)^T \Phi(\psi_t) + \Phi(\psi_t^*)^T \Phi(\psi_t^*)] y_t \quad \text{if } L_t > D_t > 0$$

Substituting (7.a) and (7.b) into this equation yields the following model for the observation vector y_t :

$$\begin{aligned} y_t &= \underline{\Phi}(\psi_t)^T \underline{\chi}_t \underline{\Phi}(\phi_t) z_t + \underline{\Phi}(\psi_t^*)^T f_t & \text{if } L_t > D_t > 0 \\ &= \underline{\Phi}(\psi_t)^T \underline{\chi}_t \underline{\Phi}(\phi_t) z_t & \text{if } L_t = D_t > 0 \\ &= \underline{\Phi}(\psi_t^*)^T f_t & \text{if } L_t > D_t = 0 \\ &= \{\} & \text{if } L_t = 0 \end{aligned} \quad (9)$$

Together with equations (3), (4), (5) and (6), equation (9) forms a complete characterization of our tracking problem in terms of stochastic difference equations.

Example: Assume we maintain tracks of five targets ($M = 5$), of which we detect and observe four ($D_t = 4$) together with two false measurements ($F_t = 2$), and with:

$$\chi_t = \begin{bmatrix} 0 & 0 & 0 & 1 \\ 0 & 0 & 1 & 0 \\ 1 & 0 & 0 & 0 \\ 0 & 1 & 0 & 0 \end{bmatrix}, \quad \phi_t = [1 \ 0 \ 1 \ 1 \ 1]^T$$

$$\psi_t = [1 \ 1 \ 0 \ 1 \ 1 \ 0]^T$$

i.e. the 2nd target is not detected, and the 3rd and 6th measurements are false. This implies:

$$\Phi(\phi_t) = \begin{bmatrix} 1 & 0 & 0 & 0 & 0 \\ 0 & 0 & 1 & 0 & 0 \\ 0 & 0 & 0 & 1 & 0 \\ 0 & 0 & 0 & 0 & 1 \end{bmatrix},$$

$$\Phi(\psi_t) = \begin{bmatrix} 1 & 0 & 0 & 0 & 0 & 0 \\ 0 & 1 & 0 & 0 & 0 & 0 \\ 0 & 0 & 0 & 1 & 0 & 0 \\ 0 & 0 & 0 & 0 & 1 & 0 \end{bmatrix},$$

$$\Phi(\psi_t^*) = \begin{bmatrix} 0 & 0 & 1 & 0 & 0 & 0 \\ 0 & 0 & 0 & 0 & 0 & 1 \end{bmatrix},$$

$$\chi_t \Phi(\phi_t) = \begin{bmatrix} 0 & 0 & 0 & 0 & 1 \\ 0 & 0 & 0 & 1 & 0 \\ 1 & 0 & 0 & 0 & 0 \\ 0 & 0 & 1 & 0 & 0 \end{bmatrix},$$

$$\underline{\Phi}(\psi_t)^T \underline{\chi}_t \underline{\Phi}(\phi_t) z_t = [z_{5,t} \ z_{4,t} \ 0 \ z_{1,t} \ z_{3,t} \ 0]^T,$$

$$\underline{\Phi}(\psi_t^*)^T f_t = [0 \ 0 \ f_{1,t} \ 0 \ 0 \ f_{2,t}]^T,$$

Substituting this in (9) yields:

$$y_t = [z_{5,t} \ z_{4,t} \ f_{1,t} \ z_{1,t} \ z_{3,t} \ f_{2,t}]^T$$

4. EXACT FILTER EQUATIONS

In this section a Bayesian characterization of the conditional density $p_{x_t, \theta_t | Y_t}(x, \theta)$ is given where Y_t denotes the σ -algebra generated by measurements y_t up to and including moment t . Subsequently, characterizations are developed for the mode probabilities and the mode conditional means and covariances. First we introduce an auxiliary indicator matrix process $\tilde{\chi}_t$ of size $D_t \times L_t$, as follows:

$$\tilde{\chi}_t \triangleq \chi_t^T \Phi(\psi_t) \quad \text{if } D_t > 0. \quad (10)$$

Pre-multiplying the left- and right hand terms in (9) with $\tilde{\chi}_t = \tilde{\chi} \otimes I_m$ and subsequent straightforward evaluation yields:

$$\tilde{\chi}_t y_t = \underline{\Phi}(\phi_t) H(\theta_t) x_t + \underline{\Phi}(\phi_t) G(\theta_t) v_t, \quad \text{if } D_t > 0, \quad (11)$$

where the size of $\tilde{\chi}_t$ is $D_t m \times L_t m$ and the size of $\underline{\Phi}(\phi_t)$ is $D_t m \times M m$.

Notice that (11) is a linear Gaussian descriptor system [19] with stochastic i.i.d. coefficients $\tilde{\chi}_t$ and $\underline{\Phi}(\phi_t)$ and Markovian switching coefficients $H(\theta_t)$ and $G(\theta_t)$.

From (11), it follows that for $D_t > 0$ all relevant associations and permutations can be covered by $(\phi_t, \tilde{\chi}_t)$ -hypotheses. We extend this to $D_t = 0$ by adding the combination $\phi_t = \{0\}^M$ and $\tilde{\chi}_t = \{\}^{L_t}$. Hence, through defining the weights

$$\beta_t(\phi, \tilde{\chi}, \theta) \triangleq \text{Prob}\{\phi_t = \phi, \tilde{\chi}_t = \tilde{\chi}, \theta_t = \theta | Y_t\},$$

the law of total probability yields:

$$p_{x_t, \theta_t | Y_t}(x, \theta) = \sum_{\tilde{\chi}, \phi} \beta_t(\phi, \tilde{\chi}, \theta) p_{x_t | \theta_t, \phi_t, \tilde{\chi}_t, Y_t}(x | \theta, \phi, \tilde{\chi}) \quad (12)$$

And thus, our problem is to characterize the terms in the last summation. This problem is solved in two steps, the first of which is the following Proposition.

Proposition 1. For any $\phi \in \{0, 1\}^M$, such that $D(\phi) \triangleq \sum_{i=1}^M \phi_i \leq L_t$, and any $\tilde{\chi}_t$ matrix realization $\tilde{\chi}$ of size $D(\phi) \times L_t$, the following holds true:

$$p_{x_t | \theta_t, \phi_t, \tilde{\chi}_t, Y_t}(x | \theta, \phi, \tilde{\chi}) = \frac{p_{\tilde{z}_t | x_t, \theta_t, \phi_t}(\tilde{\chi} Y_t | x, \theta, \phi) \cdot p_{x_t | \theta_t, Y_{t-1}}(x | \theta)}{F_t(\phi, \tilde{\chi}, \theta)} \quad (13)$$

$$\begin{aligned} \beta_t(\phi, \tilde{\chi}, \theta) &= F_t(\phi, \tilde{\chi}, \theta) \cdot \\ &\cdot \prod_{j=1}^{L_t - D(\phi)} \lambda([\Phi(1_{L_t} - \tilde{\chi}^T \tilde{\chi} 1_{L_t}) y_t]_j) \cdot \\ &\cdot \prod_{i=1}^M [(1 - P_d^i)^{(1-\phi_i)} (P_d^i)^{\phi_i}] \cdot p_{\theta_t | Y_{t-1}}(\theta) / c_t \end{aligned} \quad (14)$$

where $\tilde{\chi} \triangleq \tilde{\chi} \otimes I_m$, $1_{L_t} = [1, \dots, 1]^T$ is an L_t vector with 1-valued elements and $F_t(\phi, \tilde{\chi}, \theta)$ and c_t are such that they normalize $p_{x_t | \theta_t, \phi_t, \tilde{\chi}_t, Y_t}(x | \theta, \phi, \tilde{\chi})$ and $\beta_t(\phi, \tilde{\chi}, \theta)$ respectively.

Proof: See Appendix A

The next step starts with substituting (13) and (14) into (12), which yields:

$$\begin{aligned} p_{x_t, \theta_t | Y_t}(x, \theta) &= \\ &= \sum_{\tilde{\chi}, \phi} \left[\frac{p_{\tilde{z}_t | x_t, \theta_t, \phi_t}(\tilde{\chi} Y_t | x, \theta, \phi) \cdot p_{x_t | \theta_t, Y_{t-1}}(x | \theta)}{F_t(\phi, \tilde{\chi}, \theta)} \cdot \right. \\ &\cdot F_t(\phi, \tilde{\chi}, \theta) \cdot \prod_{j=1}^{L_t - D(\phi)} \lambda([\Phi(1_{L_t} - \tilde{\chi}^T \tilde{\chi} 1_{L_t}) y_t]_j) \cdot \\ &\cdot \left. \prod_{i=1}^M [(1 - P_d^i)^{(1-\phi_i)} (P_d^i)^{\phi_i}] \right] \cdot p_{\theta_t | Y_{t-1}}(\theta) / c_t \end{aligned}$$

Simplifying this and rearranging terms yields:

$$\begin{aligned} p_{x_t, \theta_t | Y_t}(x, \theta) &= \\ &= \sum_{\tilde{\chi}, \phi} \left[p_{\tilde{z}_t | x_t, \theta_t, \phi_t}(\tilde{\chi} Y_t | x, \theta, \phi) \cdot p_{x_t, \theta_t | Y_{t-1}}(x, \theta) \cdot \right. \\ &\cdot \prod_{j=1}^{L_t - D(\phi)} \lambda([\Phi(1_{L_t} - \tilde{\chi}^T \tilde{\chi} 1_{L_t}) y_t]_j) \cdot \\ &\cdot \left. \prod_{i=1}^M [(1 - P_d^i)^{(1-\phi_i)} (P_d^i)^{\phi_i}] / c_t \right] \end{aligned} \quad (15)$$

with

$$p_{\tilde{z}_t | x_t, \theta_t, \phi_t}(\tilde{z} | x, \theta, \phi) = N\{\tilde{z}; \Phi(\phi)H(\theta)x, \Phi(\phi)G(\theta)G(\theta)^T\Phi(\phi)^T\} \quad (16)$$

Define $\tilde{F}_t(\phi, \tilde{\chi}, x, \theta) \triangleq p_{\tilde{z}_t | x_t, \theta_t, \phi_t}(\tilde{\chi} Y_t | x, \theta, \phi)$. Hence from (16) we get:

$$\begin{aligned} \tilde{F}_t(\phi, \tilde{\chi}, x, \theta) &= [(2\pi)^{mD(\phi)} \text{Det}\{\tilde{Q}_t(\phi, \theta)\}]^{-\frac{1}{2}} \cdot \\ &\cdot \exp\{-\frac{1}{2} \tilde{v}_t^T(\phi, \tilde{\chi}, x, \theta) \tilde{Q}_t(\phi, \theta)^{-1} \tilde{v}_t(\phi, \tilde{\chi}, x, \theta)\} \end{aligned} \quad (17)$$

where

$$\begin{aligned} \tilde{v}_t(\phi, \tilde{\chi}, x, \theta) &\triangleq \tilde{\chi} y_t - \Phi(\phi)H(\theta)x \\ \tilde{Q}_t(\phi, \theta) &\triangleq \Phi(\phi)(G(\theta)G(\theta)^T)\Phi(\phi)^T \end{aligned}$$

Substituting (17) into (15) and rearranging terms yields

$$\begin{aligned} p_{x_t, \theta_t | Y_t}(x, \theta) &= \frac{1}{c_t} \sum_{\tilde{\chi}, \phi} \left[\tilde{F}_t(\phi, \tilde{\chi}, x, \theta) \cdot \right. \\ &\cdot \prod_{j=1}^{L_t - D(\phi)} \lambda([\Phi(1_{L_t} - \tilde{\chi}^T \tilde{\chi} 1_{L_t}) y_t]_j) \cdot \\ &\cdot \left. \prod_{i=1}^M [(1 - P_d^i)^{(1-\phi_i)} (P_d^i)^{\phi_i}] \right] \cdot p_{x_t, \theta_t | Y_{t-1}}(x, \theta) \end{aligned} \quad (18)$$

Theorem 1. For any $\phi \in \{0, 1\}^M$, such that $D(\phi) \triangleq \sum_{i=1}^M \phi_i \leq L_t$, the following recursive equation holds true for the conditional density $p_{x_t, \theta_t | Y_t}(x, \theta)$:

$$\begin{aligned} p_{x_t, \theta_t | Y_t}(x, \theta) &= \\ &= \frac{1}{c_t} \sum_{\phi \in \{0, 1\}^M} \left[\prod_{i=1}^M [(1 - P_d^i)^{(1-\phi_i)} (P_d^i)^{\phi_i}] \cdot \right. \\ &\cdot \sum_{\tilde{\chi}} N_{mD(\phi)}\{\tilde{\chi} y_t; \Phi(\phi)H(\theta)x, \Phi(\phi)G(\theta)G(\theta)^T\Phi(\phi)^T\} \cdot \\ &\cdot \prod_{j=1}^{L_t - D(\phi)} \lambda([\Phi(1_{L_t} - \tilde{\chi}^T \tilde{\chi} 1_{L_t}) y_t]_j) \cdot \\ &\cdot \int_{\mathbb{R}^{Mn}} N_{Mn}\{x; A(\theta)x', B(\theta)B(\theta)^T\} \cdot \\ &\cdot \sum_{\eta \in \mathbb{M}^M} [\Pi_{\eta\theta} p_{x_{t-1}, \theta_{t-1} | Y_{t-1}}(x', \eta)] dx' \end{aligned} \quad (19)$$

with normalization c_t , $N_K\{\cdot; \bar{x}, \bar{P}\}$ a K -dimensional Gaussian with mean \bar{x} and covariance \bar{P} , and 2nd sum running over all $\tilde{\chi} = \chi\Phi(\psi)$ with χ a $D(\phi) \times D(\phi)$ permutation matrix and $\psi \in \{0, 1\}^{L_t}$ such that $D(\psi) = D(\phi)$.

Proof: IMM's basic derivation [38, App. A] yields:

$$\begin{aligned} p_{x_t, \theta_t | Y_{t-1}}(x, \theta) &= \int_{\mathbb{R}^{Mn}} N_{Mn}\{x; A(\theta)x', B(\theta)B(\theta)^T\} \cdot \\ &\cdot \sum_{\eta \in \{1, \dots, N\}^M} [\Pi_{\eta\theta} p_{x_{t-1}, \theta_{t-1} | Y_{t-1}}(x', \eta)] dx' \end{aligned} \quad (20)$$

Substituting (17) and (20) in (18) and rearranging the summation over $\tilde{\chi}$ yields eq. (19). ■

Eq. (19) is a recursive equation for the exact Bayesian solution of tracking multiple targets from possibly false and missing measurements. From eq. (19) follows that if the initial density is a Gaussian mixture, then the exact conditional density solution of recursive equation (19) is a Gaussian mixture, the number of Gaussians increasing exponentially with time.

Remark 1: For jump-linear systems such recursive filter equation has been characterized by [23], and for jump-non-linear systems by [3], [16]. In [14] we provide a version of Theorem 1 under the assumption that λ is homogeneous.

Remark 2: Proposition 1 and Theorem 1 also apply when initial densities are permutation symmetric over the targets, i.e. a situation studied by [32].

5. SIR JOINT PARTICLE FILTER

In this section a SIR joint particle filter of the exact filter characterization of Theorem 1 is developed. In this SIR joint PF a particle is defined as a triplet (μ_j, x_j, θ_j) , $\mu_j \in [0, 1]$, $x_j \in \mathbb{R}^{Mn}$, $\theta_j \in \mathbb{M}^M$, $j \in [1, S]$. One filter cycle consists of the following steps:

- *SIR joint particle filter Step 0: Initiation.*

Each filter cycle starts with a set of S joint particles in $[0, 1] \times \mathbb{R}^{Mn} \times \mathbb{M}^M$, i.e.:

$$\{(\mu_{j,t-1} = 1/S, x_{j,t-1}, \theta_{j,t-1}); j \in [1, S]\}$$

with for $t = 0$, $\theta_{j,0}$ and $x_{j,0}$ independently drawn from $p_{\theta_0}(\cdot)$ and $p_{x_0|\theta_0}(\cdot|\theta_{j,0})$ respectively for each $j \in [1, S]$.

- *SIR joint particle filter Step 1: Joint mode switching.*

Determine the new joint mode per joint particle ($\mu_{j,t-1}$ and $x_{j,t-1}$ are not changed)

$$\{(\mu_{j,t-1}, x_{j,t-1}, \bar{\theta}_{j,t}); j \in [1, S]\}$$

by generating for each joint particle a new value $\bar{\theta}_{j,t}$ according to the transition probabilities:

$$\text{Prob}\{\bar{\theta}_{j,t} = \bar{\theta} \mid \theta_{j,t-1} = \theta\} = \Pi_{\theta, \bar{\theta}} \quad (21)$$

- *SIR joint particle filter Step 2: Prediction.*

Determine the new state per joint particle (the weights $\mu_{j,t-1}$ are not changed)

$$\{(\mu_{j,t-1}, \bar{x}_{j,t}, \bar{\theta}_{j,t}); j \in [1, S]\}$$

by running for each particle a Monte Carlo simulation from $(t-1)$ to t according to the model

$$\bar{x}_{j,t} = A(\bar{\theta}_{j,t})x_{j,t-1} + B(\bar{\theta}_{j,t})w_{j,t-1} \quad (22)$$

- *SIR joint particle filter Step 3: Measurement update.*

Determine new weight per joint particle, i.e.

$$\{(\bar{\mu}_{j,t}, \bar{x}_{j,t}, \bar{\theta}_{j,t}); j \in [1, S], \}$$

with for the new weights, using eqs. (17) and (18):

$$\begin{aligned} \bar{\mu}_{j,t} = & \mu_{j,t-1} \cdot \frac{1}{c_t} \sum_{\tilde{\chi}, \phi} \left[\tilde{F}_t(\phi, \tilde{\chi}, \bar{x}_{j,t}, \bar{\theta}_{j,t}) \cdot \right. \\ & \cdot \prod_{i=1}^{L_t - D(\phi)} \lambda([\Phi(1_{L_t} - \tilde{\chi}^T \tilde{\chi} 1_{L_t})y_t]_i) \cdot \\ & \left. \cdot \prod_{i=1}^M [(1 - P_d^i)^{(1-\phi_i)} (P_d^i)^{\phi_i}] \right] \quad (23) \end{aligned}$$

where

$$\begin{aligned} \tilde{F}_t(\phi, \tilde{\chi}, x, \theta) = & [(2\pi)^{mD(\phi)} \text{Det}\{\tilde{Q}_t(\phi, \theta)\}]^{-\frac{1}{2}} \cdot \\ & \cdot \exp\left\{-\frac{1}{2} \tilde{\nu}_t^T(\phi, \tilde{\chi}, x, \theta) \tilde{Q}_t(\phi, \theta)^{-1} \tilde{\nu}_t(\phi, \tilde{\chi}, x, \theta)\right\} \quad (24) \end{aligned}$$

with

$$\begin{aligned} \tilde{\nu}_t(\phi, \tilde{\chi}, x, \theta) & \triangleq \tilde{\chi}y_t - \underline{\Phi}(\phi)H(\theta)x \\ \tilde{Q}_t(\phi, \theta) & \triangleq \underline{\Phi}(\phi)(G(\theta)G(\theta)^T)\underline{\Phi}(\phi)^T \end{aligned}$$

and c_t a normalizing constant such that

$$\sum_{j=1}^S \bar{\mu}_{j,t} = 1$$

- *SIR joint particle filter Step 4: MMSE output equations:*

$$\hat{\gamma}_t(\theta) = \sum_{j=1}^S \bar{\mu}_{j,t} 1_{\bar{\theta}_{j,t}}(\theta)$$

$$\hat{x}_t(\theta) = \sum_{j=1}^S \bar{\mu}_{j,t} \bar{x}_{j,t} 1_{\bar{\theta}_{j,t}}(\theta)$$

$$\hat{P}_t(\theta) = \sum_{j=1}^S \bar{\mu}_{j,t} [\bar{x}_{j,t} - \hat{x}_t(\theta)][\bar{x}_{j,t} - \hat{x}_t(\theta)]^T 1_{\bar{\theta}_{j,t}}(\theta)$$

$$\hat{x}_t = \sum_{\theta \in \mathbb{M}^M} \hat{\gamma}(\theta) \hat{x}_t(\theta)$$

$$\hat{P}_t = \sum_{\theta \in \mathbb{M}^M} \hat{\gamma}(\theta) \left(\hat{P}_t(\theta) + [\hat{x}_t(\theta) - \hat{x}_t][\hat{x}_t(\theta) - \hat{x}_t]^T \right)$$

- *SIR joint particle filter Step 5: Resampling.*

Generate the new set of joint particles

$$\{(\mu_{j,t} = 1/S, x_{j,t}, \theta_{j,t}); j \in [1, S]\}$$

with $\theta_{j,t}$ and $x_{j,t}$ the j -th of the S samples drawn independently from the joint particle spanned conditional densities for θ_t given y_t and for x_t given Y_t and $\theta_t = \theta_{j,t}^j$:

$$p_{\theta_t|Y_t}(\theta) \approx \hat{\gamma}_t(\theta)$$

$$p_{x_t|\theta_t, Y_t}(\cdot|\theta_{j,t}) \approx \sum_{l=1}^S \bar{\mu}_{l,t} 1_{\bar{\theta}_{l,t}}(\theta_{j,t}) \delta_{\bar{x}_{l,t}}(\cdot)$$

In the next section we modify the enumeration of the particles and adopt the particle resampling step 5.

6. HYBRID SIR JOINT PARTICLE FILTER

In this section a hybrid SIR joint particle filter of the exact filter characterization of Theorem 1 is developed. The difference with the SIR joint particle filter is that we now resample a fixed number of joint particles per joint mode. A joint particle is defined as a triplet $(\mu^{\theta,j}, x^{\theta,j}, \theta)$, $\mu^{\theta,j} \in [0, 1]$, $x^{\theta,j} \in \mathbb{R}^{Mn}$, $\theta \in \mathbb{M}^M$, $j \in [1, S']$. One cycle of this hybrid SIR joint particle filter consists of the following steps:

- *Hybrid SIR joint particle filter Step 0: Initiation.*

Each filter cycle starts with a set of $S = NS'$ joint particles in $[0, 1] \times \mathbb{R}^{Mn} \times \mathbb{M}^M$, i.e.:

$$\{(\mu_{t-1}^{\theta,j}, x_{t-1}^{\theta,j}, \theta_{t-1}^{\theta,j} = \theta); j \in [1, S'], \theta \in \mathbb{M}^M\}$$

with for $t = 0$, $\mu_0^{\theta,j} = p_{\theta_0}(\theta)/S'$, and $x_0^{\theta,j}$ independently drawn from $p_{x_0|\theta_0}(\cdot|\theta)$ for each $j \in 1, \dots, S'$.

- *Hybrid SIR joint particle filter Step 1: Mode switching.*

Determine the new mode per particle ($\mu_{t-1}^{\theta,j}$ and $x_{t-1}^{\theta,j}$ are not changed)

$$\{(\mu_{t-1}^{\theta,j}, x_{t-1}^{\theta,j}, \bar{\theta}_t^{\theta,j}); j \in [1, S'], \theta \in \mathbb{M}^M\}$$

by generating for each joint particle a new value $\bar{\theta}_t^{\theta,j}$ according to the model

$$\text{Prob}\{\bar{\theta}_t^{\theta,j} = \bar{\theta} \mid \theta_{t-1}^{\theta,j} = \theta\} = \Pi_{\theta, \bar{\theta}} \quad (25)$$

- *Hybrid SIR joint particle filter Step 2: Prediction.*

Determine the new state per joint particle (the weights $\mu_{t-1}^{\theta,j}$ are not changed)

$$\{(\mu_{t-1}^{\theta,j}, \bar{x}_t^{\theta,j}, \bar{\theta}_t^{\theta,j}); j \in [1, S'], \theta \in \mathbb{M}^M\}$$

by running for each particle a Monte Carlo simulation from $(t-1)$ to t according to the model

$$\bar{x}_t^{\theta,j} = A(\bar{\theta}_t^{\theta,j})x_{t-1}^{\theta,j} + B(\bar{\theta}_t^{\theta,j})w_{t-1} \quad (26)$$

- *Hybrid SIR joint particle filter Step 3: Measurement update.*

Determine new weight per joint particle, i.e.

$$\{(\bar{\mu}_t^{\theta,j}, \bar{x}_t^{\theta,j}, \bar{\theta}_t^{\theta,j}); j \in [1, S'], \theta \in \mathbb{M}^M\}$$

with for the new weights, using eqs. (17) and (18):

$$\begin{aligned} \bar{\mu}_t^{\theta,j} &= \mu_{t-1}^{\theta,j} \cdot \frac{1}{c_t} \sum_{\tilde{x}, \phi} \left[\tilde{F}_t(\phi, \tilde{x}, \bar{x}_t^{\theta,j}, \bar{\theta}_t^{\theta,j}) \cdot \right. \\ &\quad \cdot \prod_{i=1}^{L_t-D(\phi)} \lambda([\Phi(1_{L_t} - \tilde{\chi}^T \tilde{\chi} 1_{L_t})y_t]_i) \cdot \\ &\quad \left. \cdot \prod_{i=1}^M [(1 - P_d^i)^{(1-\phi_i)} (P_d^i)^{\phi_i}] \right] \quad (27) \end{aligned}$$

where

$$\begin{aligned} \tilde{F}_t(\phi, \tilde{x}, x, \theta) &= [(2\pi)^{mD(\phi)} \text{Det}\{\tilde{Q}_t(\phi, \theta)\}]^{-\frac{1}{2}} \cdot \\ &\cdot \exp\{-\frac{1}{2} \tilde{\nu}_t^T(\phi, \tilde{x}, x, \theta) \tilde{Q}_t(\phi, \theta)^{-1} \tilde{\nu}_t(\phi, \tilde{x}, x, \theta)\} \quad (28) \end{aligned}$$

with

$$\begin{aligned} \tilde{\nu}_t(\phi, \tilde{x}, x, \theta) &\triangleq \tilde{\chi}y_t - \Phi(\phi)H(\theta)x \\ \tilde{Q}_t(\phi, \theta) &\triangleq \Phi(\phi)(G(\theta)G(\theta)^T)\Phi(\phi)^T \end{aligned}$$

and c_t a normalizing constant such that

$$\sum_{\theta \in \mathbb{M}^M} \sum_{j=1}^{S'} \bar{\mu}_t^{\theta,j} = 1$$

- *Hybrid SIR joint particle filter Step 4: MMSE output equations:*

$$\hat{\gamma}_t(\theta) = \sum_{\eta \in \mathbb{M}^M} \sum_{j=1}^{S'} \bar{\mu}_t^{\eta,j} 1_{\bar{\theta}_t^{\eta,j}}(\theta)$$

$$\hat{x}_t(\theta) = \sum_{\eta \in \mathbb{M}^M} \sum_{j=1}^{S'} \bar{\mu}_t^{\eta,j} \bar{x}_t^{\eta,j} 1_{\bar{\theta}_t^{\eta,j}}(\theta)$$

$$\hat{P}_t(\theta) = \sum_{\eta \in \mathbb{M}^M} \sum_{j=1}^{S'} \bar{\mu}_t^{\eta,j} [\bar{x}_t^{\eta,j} - \hat{x}_t(\theta)][\bar{x}_t^{\eta,j} - \hat{x}_t(\theta)]^T 1_{\bar{\theta}_t^{\eta,j}}(\theta)$$

$$\hat{x}_t = \sum_{\theta \in \mathbb{M}^M} \hat{\gamma}_t(\theta) \hat{x}_t(\theta)$$

$$\hat{P}_t = \sum_{\theta \in \mathbb{M}^M} \hat{\gamma}_t(\theta) \left(\hat{P}_t(\theta) + [\hat{x}_t(\theta) - \hat{x}_t][\hat{x}_t(\theta) - \hat{x}_t]^T \right)$$

- *Hybrid SIR joint particle filter Step 5: Resampling per mode.*

Generate the new set of joint particles

$$\{(\mu_t^{\theta,j} = \hat{\gamma}_t(\theta)/S', x_t^{\theta,j}, \theta_t^{\theta,j} = \theta); j \in [1, S'], \theta \in \mathbb{M}^M\}$$

with $x_t^{\theta,j}$ the j -th of the S' samples drawn independently from the particle spanned conditional density for x_t given Y_t and $\theta_t = \theta$:

$$p_{x_t|\theta_t, Y_t}(\cdot|\theta) \approx \sum_{\eta \in \mathbb{M}^M} \sum_{l=1}^{S'} \bar{\mu}_t^{\eta,l} 1_{\bar{\theta}_t^{\eta,l}}(\theta) \delta_{\bar{x}_t^{\eta,l}}(x)$$

For homogeneous λ , this hybrid SIR joint particle filter has been introduced in [11] under the name Joint IMMPPDA particle filter.

7. IMMJPDA ASSUMPTIONS

The assumptions that are underlying to the IMMJPDA of [18] are:

- C1) $p_{\theta_t|Y_{t-1}}(\theta) = \prod_{i=1}^M p_{\theta_t^i|Y_{t-1}}(\theta^i)$;
- C2) $p_{x_t|\theta_t, Y_{t-1}}(x|\theta) = \prod_{i=1}^M p_{x_t^i|\theta_t^i, Y_{t-1}}(x^i|\theta^i)$;
- C3) $p_{x_t^i|\theta_t^i, Y_{t-1}}(x^i|\theta^i)$ is Gaussian with mean $\bar{x}_t^i(\theta^i)$ and covariance $P_t^i(\theta^i)$

Application of these assumptions, to the exact equations of Proposition 1 yields the following theorem.

Theorem 2. Assume C1, C2 and C3 are satisfied. Then $\beta_t(\phi, \tilde{\chi}, \theta)$ of Proposition 1 satisfies:

$$\beta_t(\phi, \tilde{\chi}, \theta) = \left[\prod_{i=1}^{L_t - D(\phi)} \lambda([\Phi(1_{L_t} - \tilde{\chi}^T \tilde{\chi} 1_{L_t}) y_t]_i) \right] \cdot \prod_{i=1}^M \left[f_t^i(\phi, \tilde{\chi}, \theta^i) (1 - P_d^i)^{(1 - \phi_i)} (P_d^i)^{\phi_i} \cdot p_{\theta_t^i | Y_{t-1}}(\theta^i) \right] / c_t \quad (29)$$

with for $\phi^i = 0$: $f_t^i(\phi, \tilde{\chi}, \theta^i) = 1$, and for $\phi^i = 1$:

$$f_t^i(\phi, \tilde{\chi}, \theta^i) = [(2\pi)^m \text{Det}\{\bar{Q}_t^i(\theta^i)\}]^{-\frac{1}{2} \phi_i} \cdot \exp\left\{-\frac{1}{2} \sum_{k=1}^{L_t} ([\Phi(\phi)^T]_{i*} \tilde{\chi}_{*k} \nu_t^{ik}(\theta^i)^T [\bar{Q}_t^i(\theta^i)]^{-1} \nu_t^{ik}(\theta^i))\right\} \quad (30.a)$$

$$\nu_t^{ik}(\theta^i) = y_t^k - h^i(\theta^i) \bar{x}_t^i(\theta^i) \quad (30.b)$$

$$\bar{Q}_t^i(\theta^i) = h^i(\theta^i) \bar{P}_t^i(\theta^i) h^i(\theta^i)^T + g^i(\theta^i) g^i(\theta^i)^T \quad (30.c)$$

where $[\Phi(\phi)^T]_{i*}$ and $\tilde{\chi}_{*k}$ are the i -th row and k -th column of $\Phi(\phi)^T$ and $\tilde{\chi}$, respectively. Moreover, $p_{x_t^i | \theta_t^i, Y_t}(x^i | \theta^i)$, $i \in [1, M]$, is a Gaussian mixture, while its overall mean $\hat{x}_t^i(\theta^i)$ and its overall covariance $\hat{P}_t^i(\theta^i)$ satisfy:

$$p_{\theta_t^i | Y_t}(\theta^i) = \sum_{\substack{\phi, \tilde{\chi}, \eta \\ \eta^i = \theta^i}} \beta_t(\phi, \tilde{\chi}, \eta) \quad (31.a)$$

$$\hat{x}_t^i(\theta^i) = \bar{x}_t^i(\theta^i) + W_t^i(\theta^i) \left(\sum_{k=1}^{L_t} \beta_t^{ik}(\theta^i) \nu_t^{ik}(\theta^i) \right) \quad (31.b)$$

$$\begin{aligned} \hat{P}_t^i(\theta^i) &= \bar{P}_t^i(\theta^i) - W_t^i(\theta^i) h^i(\theta^i) \bar{P}_t^i(\theta^i) \left(\sum_{k=1}^{L_t} \beta_t^{ik}(\theta^i) \right) + \\ &+ W_t^i(\theta^i) \left(\sum_{k=1}^{L_t} \beta_t^{ik}(\theta^i) \nu_t^{ik}(\theta^i) \nu_t^{ik}(\theta^i)^T \right) W_t^i(\theta^i)^T + \\ &- W_t^i(\theta^i) \left(\sum_{k=1}^{L_t} \beta_t^{ik}(\theta^i) \nu_t^{ik}(\theta^i) \right) \cdot \\ &\cdot \left(\sum_{k'=1}^{L_t} \beta_t^{ik'}(\theta^i) \nu_t^{ik'}(\theta^i) \right)^T W_t^i(\theta^i)^T \end{aligned} \quad (31.c)$$

with:

$$W_t^i(\theta^i) = \bar{P}_t^i(\theta^i) h^i(\theta^i)^T [\bar{Q}_t^i(\theta^i)]^{-1} \quad (31.d)$$

$$\begin{aligned} \beta_t^{ik}(\theta^i) &\triangleq \text{Prob}\{[\Phi(\phi)^T]_{i*} [\tilde{\chi}]_{*k} = 1 \mid \theta_t^i = \theta^i, Y_t\} = \\ &= \sum_{\substack{\phi, \tilde{\chi}, \eta \\ \phi \neq 0 \\ \eta^i = \theta^i}} [\Phi(\phi)^T]_{i*} \tilde{\chi}_{*k} \beta_t(\phi, \tilde{\chi}, \eta) / p_{\theta_t^i | Y_t}(\theta^i) \end{aligned} \quad (31.e)$$

Proof: See Appendix B. ■

Eq. (30a) replaces six nested equations of [18, eqs. (18) and (20)-(24)]. As a direct consequence, Theorem 2 leads to a more compact version of IMMJPDA, the detailed steps of which we give in the next section.

8. TRACK-COALESCENCE-AVOIDING IMMJPDA FILTER

Fitzgerald [24] has shown that less likely permutation hypotheses pruning provides an effective strategy towards reducing JPDA's sensitivity to track coalescence if $\lambda = 0$ and $P_d^i = 1$. In [8] we have shown that for $\lambda > 0$ or $P_d^i < 1$, the appropriate strategy is to prune per (ϕ_t, ψ_t) -hypothesis all but the most likely χ_t -hypothesis prior to measurement updating. This hypothesis pruning strategy is now extended as follows: evaluate all $(\phi_t, \psi_t, \theta_t)$ hypotheses and prune per $(\phi_t, \psi_t, \theta_t)$ -hypothesis all but the most-likely χ_t -hypothesis. For every ϕ , ψ and θ , satisfying $D(\psi) = D(\phi) \leq \text{Min}\{M, L_t\}$, the most likely χ hypothesis satisfies the mapping $\hat{\chi}_t(\phi, \psi, \theta)$:

$$\hat{\chi}_t(\phi, \psi, \theta) \triangleq \underset{\chi}{\text{Argmax}} \beta_t(\phi, \chi^T \Phi(\psi), \theta)$$

where the maximization is over all permutation matrices χ of size $D(\phi) \times D(\phi)$.

The pruning strategy of evaluating all (ϕ, ψ, θ) -hypotheses and only one χ -hypothesis per (ϕ, ψ, θ) -hypothesis implies that we adopt the following pruned hypothesis weights $\hat{\beta}_t(\phi, \psi, \theta)$:

$$\begin{aligned} \hat{\beta}_t(\phi, \psi, \theta) &= \beta_t(\phi, \hat{\chi}(\phi, \psi, \theta)^T \Phi(\psi), \theta) / \hat{c}_t \\ &= \beta_t(\{0\}^M, \{\}^{L_t}, \theta) / \hat{c}_t \quad \text{if } 0 < D(\phi) \leq \text{Min}\{M, L_t\} \\ &= 0 \quad \text{if } D(\phi) = 0 \\ &= 0 \quad \text{else} \end{aligned}$$

with \hat{c}_t a normalization constant for $\hat{\beta}_t$; i.e. such that

$$\sum_{D(\psi)=D(\phi)} \hat{\beta}_t(\phi, \psi, \theta) = 1$$

Through combining the equations of Theorem 2 with the above step, we arrive at the track-coalescence-avoiding IMMJPDA, for short IMMJPDA*:

IMMJPDA* Step 1: For each target this comes down to the interaction step of the IMM algorithm [7] for all $i \in [1, M]$: Starting with

$$\hat{\gamma}_{t-1}^i(\theta^i) \triangleq p_{\theta_{t-1}^i | Y_{t-1}}(\theta^i), \quad \theta^i \in \mathbb{M}$$

$$\hat{x}_{t-1}^i(\theta^i) \triangleq E\{x_{t-1}^i | \theta_{t-1}^i = \theta^i, Y_{t-1}\}, \quad \theta^i \in \mathbb{M}$$

$$\hat{P}_{t-1}^i(\theta^i) \triangleq E\{[x_{t-1}^i - \hat{x}_{t-1}^i(\theta^i)][x_{t-1}^i - \hat{x}_{t-1}^i(\theta^i)]^T \mid \theta_{t-1}^i = \theta^i, Y_{t-1}\}, \quad \theta^i \in \mathbb{M}$$

one evaluates the mixed initial condition for the filter matched to $\theta_t^i = \theta^i$ as follows (due to eq. (4)):

$$\begin{aligned} \tilde{\gamma}_t^i(\theta^i) &= \sum_{\eta^i=1}^N \Pi_{\eta^i, \theta^i}^i \cdot \hat{\gamma}_{t-1}^i(\eta^i) \\ \hat{x}_{t-1}^i | \theta_t^i(\theta^i) &= \sum_{\eta^i=1}^N \Pi_{\eta^i, \theta^i}^i \cdot \hat{\gamma}_{t-1}^i(\eta^i) \cdot \hat{x}_{t-1}^i(\eta^i) / \tilde{\gamma}_t^i(\theta^i) \\ \hat{P}_{t-1}^i | \theta_t^i(\theta^i) &= \sum_{\eta^i=1}^N \Pi_{\eta^i, \theta^i}^i \cdot \hat{\gamma}_{t-1}^i(\eta^i) \cdot \\ &\cdot \left(\hat{P}_{t-1}^i(\eta^i) + [\hat{x}_{t-1}^i(\eta^i) - \hat{x}_{t-1}^i | \theta_t^i(\theta^i)] \cdot \right. \\ &\quad \left. \cdot [\hat{x}_{t-1}^i(\eta^i) - \hat{x}_{t-1}^i | \theta_t^i(\theta^i)]^T \right) / \tilde{\gamma}_t^i(\theta^i) \end{aligned}$$

IMMJPDA* Step 2: Prediction for all $i \in [1, M]$, $\theta^i \in \mathbb{M}$:

$$\bar{x}_t^i(\theta^i) = a^i(\theta^i)\hat{x}_{t-1|\theta_t^i}^i(\theta^i) \quad (32.a)$$

$$\bar{P}_t^i(\theta^i) = a^i(\theta^i)\bar{P}_{t-1|\theta_t^i}^i(\theta^i)a^{i^T}(\theta^i) + b^i(\theta^i)b^{i^T}(\theta^i) \quad (32.b)$$

$$\bar{Q}_t^i(\theta^i) = h^i(\theta^i)\bar{P}_t^i(\theta^i)h^{i^T}(\theta^i) + g^i(\theta^i)g^{i^T}(\theta^i) \quad (32.c)$$

IMMJPDA* Step 3: Gating, which is based on [5].

Identify for each target the mode for which $\text{Det } \bar{Q}_t^i(\theta)$ is largest:

$$\theta_t^{*i} = \text{Argmax}_{\theta} \{\text{Det } \bar{Q}_t^i(\theta)\}$$

and use this to define for each target i a gate $G_t^i \in \mathbb{R}^m$ as follows:

$$G_t^i \triangleq \{z^i \in \mathbb{R}^m; [z^i - h^i(\theta_t^{*i})\bar{x}_t^i(\theta_t^{*i})]^T \cdot \bar{Q}_t^i(\theta_t^{*i})^{-1}[z^i - h^i(\theta_t^{*i})\bar{x}_t^i(\theta_t^{*i})] \leq \kappa\}$$

with κ the gate size. Now we define L_t to denote the number of measurements y_t that are in one or more of the gates G_t^i .

IMMJPDA* Step 4: Evaluation of the detection/association/mode hypotheses is based on Theorem 2; for all $\phi \in \{0, 1\}^M$, $\tilde{\chi} \in \{0, 1\}^{D(\phi) \times L_t}$, $\theta \in \mathbb{M}^M$,

$$\begin{aligned} \beta_t(\phi, \tilde{\chi}, \theta) &\cong \left[\prod_{i=1}^{L_t - D(\phi)} \lambda([\Phi(1_{L_t} - \tilde{\chi}^T \tilde{\chi} 1_{L_t})y_t]_i) \right] \cdot \\ &\cdot \prod_{i=1}^M [f_t^i(\phi, \tilde{\chi}, \theta^i) \cdot \bar{\gamma}_t^i(\theta^i)] \cdot \\ &\cdot (1 - P_d^i \text{Chi}_m^2(\kappa))^{(1-\phi_i)} (P_d^i \text{Chi}_m^2(\kappa))^{\phi_i} / c_t \\ &\quad \text{if } \tilde{\chi} 1_{L_t} = 1_{D(\phi)}, \\ &= 0 \quad \text{else} \end{aligned} \quad (33.a)$$

with for $\phi^i = 0$: $f_t^i(\phi, \tilde{\chi}, \theta^i) = 1$, and for $\phi^i = 1$:

$$\begin{aligned} f_t^i(\phi, \tilde{\chi}, \theta^i) &\cong [(2\pi)^m \text{Det}\{\bar{Q}_t^i(\theta^i)\}]^{-\frac{1}{2}\phi_i} \cdot \\ &\cdot \exp\left\{-\frac{1}{2} \sum_{k=1}^{L_t} [\Phi(\phi)^T]_{i*} \tilde{\chi}_{*k} \nu_t^{ik}(\theta^i)^T [\bar{Q}_t^i(\theta^i)]^{-1} \nu_t^{ik}(\theta^i)\right\} \end{aligned} \quad (33.b)$$

$$\nu_t^{ik}(\theta^i) = y_t^k - h^i(\theta^i)\bar{x}_t^i(\theta^i) \quad (33.c)$$

IMMJPDA* Step 5: Track-coalescence hypothesis pruning.

First evaluate for every (ϕ, ψ, θ) such that $0 < D(\psi) = D(\phi) \leq \text{Min}\{M, L_t\}$:

$$\hat{\chi}_t(\phi, \psi, \theta) \triangleq \text{Argmax}_{\chi} \beta_t(\phi, \chi^T \Phi(\psi), \theta)$$

Next evaluate all $\hat{\chi}_t(\phi, \psi, \theta)$ hypothesis weights:

$$\begin{aligned} \hat{\beta}_t(\phi, \psi, \theta) &= \beta_t(\phi, \hat{\chi}_t(\phi, \psi, \theta)^T \Phi(\psi), \theta) / \hat{c}_t \\ &\quad \text{if } 0 < D(\psi) = D(\phi) \leq \text{Min}\{M, L_t\} \\ &= \beta_t(\{0\}^M, \{\}^{L_t}, \theta) / \hat{c}_t \\ &\quad \text{if } D(\psi) = D(\phi) = 0 \\ &= 0 \quad \text{else} \end{aligned}$$

where \hat{c}_t is a normalizing constant for $\hat{\beta}_t$.

IMMJPDA* Step 6: Measurement update equations (also based on Theorem 2); for all $i \in [1, M]$, $\theta^i \in \mathbb{M}$,

$$\hat{\gamma}_t^i(\theta^i) \cong \sum_{\substack{\phi, \psi, \eta \\ \eta^i = \theta^i}} \hat{\beta}_t(\phi, \psi, \eta) \quad (34.a)$$

$$\hat{x}_t^i(\theta^i) \cong \bar{x}_t^i(\theta^i) + W_t^i(\theta^i) \left(\sum_{k=1}^{L_t} \hat{\beta}_t^{ik}(\theta^i) \nu_t^{ik}(\theta^i) \right) \quad (34.b)$$

$$\begin{aligned} \hat{P}_t^i(\theta^i) &\cong \bar{P}_t^i(\theta^i) - W_t^i(\theta^i) h^i(\theta^i) \bar{P}_t^i(\theta^i) \left(\sum_{k=1}^{L_t} \hat{\beta}_t^{ik}(\theta^i) \right) \\ &+ W_t^i(\theta^i) \left(\sum_{k=1}^{L_t} \hat{\beta}_t^{ik}(\theta^i) \nu_t^{ik}(\theta^i) \nu_t^{ik}(\theta^i)^T \right) W_t^i(\theta^i)^T \\ &- W_t^i(\theta^i) \left(\sum_{k=1}^{L_t} \hat{\beta}_t^{ik}(\theta^i) \nu_t^{ik}(\theta^i) \right) \cdot \\ &\cdot \left(\sum_{k'=1}^{L_t} \hat{\beta}_t^{ik'}(\theta^i) \nu_t^{ik'}(\theta^i) \right)^T W_t^i(\theta^i)^T \end{aligned} \quad (34.c)$$

with:

$$W_t^i(\theta^i) = \bar{P}_t^i(\theta^i) h^i(\theta^i)^T [\bar{Q}_t^i(\theta^i)]^{-1} \quad (34.d)$$

$$\begin{aligned} \hat{\beta}_t^{ik}(\theta^i) &= \left(\sum_{\substack{\phi, \psi, \eta \\ \phi, \psi \neq 0 \\ \eta^i = \theta^i}} [\Phi(\phi)^T]_{i*} [\hat{\chi}_t(\phi, \psi, \eta)^T \Phi(\psi)]_{*k} \cdot \right. \\ &\quad \left. \hat{\beta}_t(\phi, \psi, \eta) \right) / \hat{\gamma}_t^i(\theta^i) \end{aligned} \quad (34.e)$$

where $[\cdot]_{*k}$ is the k -th column of $[\cdot]$ and $[\cdot]_{i*}$ is the i -th row of $[\cdot]$.

IMMJPDA* Step 7: Output equations:

$$\hat{x}_t^i = \sum_{\theta^i=1}^N \hat{\gamma}_t^i(\theta^i) \cdot \hat{x}_t^i(\theta^i) \quad (35.a)$$

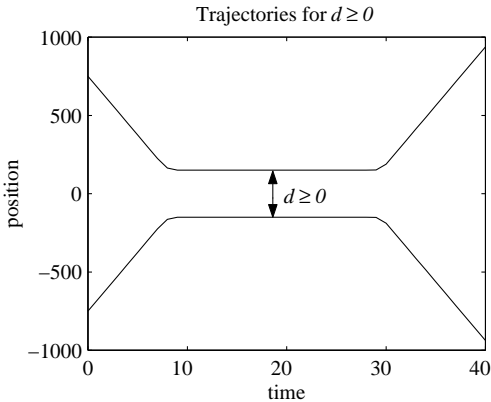
$$\hat{P}_t^i = \sum_{\theta^i=1}^N \hat{\gamma}_t^i(\theta^i) (\hat{P}_t^i(\theta^i) + [\hat{x}_t^i(\theta^i) - \hat{x}_t^i] \cdot [\hat{x}_t^i(\theta^i) - \hat{x}_t^i]^T) \quad (35.b)$$

Remark 3: By deleting the track coalescence hypothesis pruning step 5 from IMMJPDA*, and by replacing $\hat{\beta}(\phi, \psi, \eta)$ by $\beta(\phi, \psi, \eta)$ in steps 6 and 7, we get the compact IMMJPDA filter. As already announced in remark 2, the reason to refer to compact IMMJPDA is that equation (33.b) replaces six nested equations in the IMMJPDA of [18, eqs. (18) and (20)-(24)].

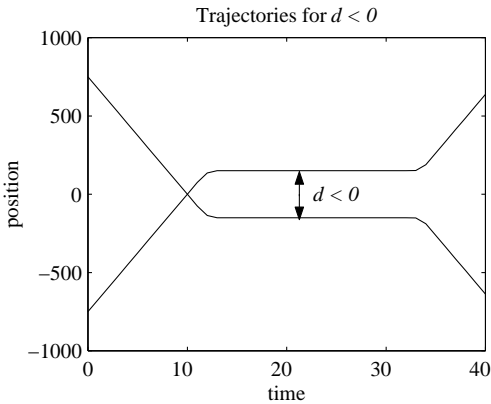
9. MONTE CARLO SIMULATIONS

In this section some Monte Carlo simulation results are given for the two novel joint particle filters, for the (compact) IMMJPDA and IMMJPDA* filter algorithms, and for a multi target tracker using an IMM-PDA for each track. The two particle filters ran on a total of $S = 10^4$ joint particles. The simulations aim at gaining insight into the behavior and performance of the filters regarding track maintenance when

two targets move in and out close approach situations, while giving the filters enough time to converge after a manoeuvre has taken place. In the example scenarios there are two tracked targets, each modeled with two possible modes. The first mode represents a constant velocity model and the second mode represents a constant acceleration model. It is assumed that both targets are initially tracked well, that for their initial track estimates there is no uncertainty regarding which track belongs to which target. Both objects move towards each other, each with constant initial velocity V_{initial} . At a certain moment in time both objects start decelerating with -50 m/s^2 until they both have zero velocity. The moment at which the deceleration starts is such that when the objects both have zero velocity, the distance between the two objects equals d (see figure 1). After spending a significant number of scans with zero velocity, both objects start accelerating with 50 m/s^2 away from each other without crossing until their velocity equals the opposite of their initial velocity. From that moment on the velocity of both objects remains constant again (thus the final relative velocity $V_{\text{rel, final}} = V_{\text{rel, initial}}$). Note that $d < 0$ implies that the objects have crossed each other before they have reached zero velocity. Each simulation the filters start with perfect estimates and run for 40 scans. Examples of the trajectories for $d \geq 0$ and $d < 0$ are depicted in figures 1a and 1b respectively.



1a. Trajectories examples for $d \geq 0$



1b. Trajectories examples for $d < 0$

Fig. 1. Trajectories examples for $d \geq 0$ and for $d < 0$

For each target, the underlying model of the potential target

measurements is given by (1) and (2), i.e.:

$$\begin{aligned} x_{t+1}^i &= a^i(\theta_{t+1}^i)x_t^i + b^i(\theta_{t+1}^i)w_t^i \\ z_t^i &= h^i(\theta_t^i)x_t^i + g^i(\theta_t^i)v_t^i \end{aligned}$$

with for $i \in \{1, 2\}$ and $\theta_t^i \in \{1, 2\}$:

$$\begin{aligned} a^i(1) &= \begin{bmatrix} 1 & T_s & 0 \\ 0 & 1 & 0 \\ 0 & 0 & 0 \end{bmatrix}, & a^i(2) &= \begin{bmatrix} 1 & T_s & \frac{1}{2}T_s^2 \\ 0 & 1 & T_s \\ 0 & 0 & 1 \end{bmatrix} \\ b^i(1) &= \sigma_a^i \cdot \begin{bmatrix} 0 \\ 0 \\ 1 \end{bmatrix}, & b^i(2) &= \sigma_a^i \cdot \begin{bmatrix} 0 \\ 0 \\ 0 \end{bmatrix} \\ h^i &= \begin{bmatrix} 1 & 0 & 0 \end{bmatrix}, & g^i &= \sigma_m^i \\ \Pi &= \begin{bmatrix} 1 - T_s/\tau_1 & T_s/\tau_1 \\ T_s/\tau_2 & 1 - T_s/\tau_2 \end{bmatrix} \end{aligned}$$

where σ_a^i represents the standard deviation of acceleration noise and σ_m^i represents the standard deviation of the measurement error. For simplicity we consider the situation of similar targets only; i.e. $\sigma_a^i = \sigma_a$, $\sigma_m^i = \sigma_m$, $P_d^i = P_d$. With this, the scenario parameters are P_d , λ , d , V_{initial} , T_s , σ_m , σ_a , τ_1 , τ_2 , and the gate size γ . We used fixed parameters $\sigma_m = 30$, $\sigma_a = 50$, $\tau_1 = 50$, $\tau_2 = 5$, and $\gamma = 25$. Table 1 gives the other scenario parameter values that are being used for the Monte Carlo simulations.

TABLE I
SCENARIO PARAMETER VALUES¹.

Scenario	P_d	λ	d	V_{initial}	T_s
1	1	0	Variable	75	1
2	1	0.001	Variable	75	1
3	0.9	0	Variable	75	1
4	0.9	0.001	Variable	75	1

During our simulations we counted track i "OK", if

$$|h^i \hat{x}_T^i - h^i x_T^i| \leq 9\sigma_m$$

and we counted track $i \neq j$ "Swapped", if

$$|h^i \hat{x}_T^i - h^j x_T^j| \leq 9\sigma_m$$

Furthermore, two tracks $i \neq j$ are counted "Coalescing" at scan t , if

$$|h^i \hat{x}_t^i - h^j \hat{x}_t^j| \leq \sigma_m \wedge |h^i x_t^i - h^j x_t^j| > \sigma_m$$

For each of the scenarios Monte Carlo simulations containing 100 runs have been performed for each of the tracking filters.

¹IMPPDA's $\lambda = 0.00001$ for scenarios 1 and 3

The initial track estimates are

$$\hat{x}_0^1(\theta) = \begin{bmatrix} -750 \\ 75 \\ 0 \end{bmatrix}, \quad \hat{x}_0^2(\theta) = \begin{bmatrix} 750 \\ -75 \\ 0 \end{bmatrix}, \quad \theta \in \{1, 2\}$$

$$\hat{P}_0^i(1) = \begin{bmatrix} 100 & 0 & 0 \\ 0 & \frac{100}{9} & 0 \\ 0 & 0 & \frac{1}{9} \end{bmatrix}, \quad \hat{P}_0^i(2) = \begin{bmatrix} 100 & 0 & 0 \\ 0 & \frac{100}{9} & 0 \\ 0 & 0 & \frac{1}{36} \end{bmatrix}$$

$$\hat{\gamma}_0^i(1) = 0.9, \quad \hat{\gamma}_0^i(2) = 0.1, \quad \text{for } i = 1, 2$$

The results of the Monte Carlo simulations for the four scenarios are shown in tables and figures as follows:

- The percentage of Both tracks "OK", see Table II, and figures 2a, 3a, 4a and 5a.
- The percentage of Both tracks "OK" or "Swapped", see Table III, and figures 2b, 3b, 4b and 5b.
- The average number of "coalescing" scans, see Table IV, and figures 2c, 3c, 4c and 5c.
- The average CPU time per scan (in seconds), see Table V.

TABLE II
AVERAGE % BOTH TRACKS "OK".

Sc.	IMMPDA	IMMJFDA	IMMJFDA*	SIR joint	SIR-H joint
1	19	66	73	70	75
2	10	56	68	65	70
3	6	63	69	70	72
4	4	41	50	43	57

TABLE III
AVERAGE % BOTH TRACKS "OK" OR "SWAPPED".

Sc.	IMMPDA	IMMJFDA	IMMJFDA*	SIR joint	SIR-H joint
1	28.3	99.96	100	97.8	96.2
2	18.9	92.5	96.8	91.6	94.6
3	8.5	99.8	100	97.6	95.8
4	5.6	76.6	80.96	66.0	82.3

TABLE IV
AVERAGE NUMBER OF COALESCING SCANS.

Sc.	IMMPDA	IMMJFDA	IMMJFDA*	SIR joint	SIR-H joint
1	9.7	1.5	0.4	1.2	1.3
2	11.0	2.1	0.3	1.2	1.4
3	18.9	1.7	0.5	1.3	1.3
4	14.5	2.6	0.5	1.3	1.5

The results in Tables II-IV and figures 2-5 show that for targets that come close to each other, IMMJFDA, IMMJFDA* and the particle filters perform much better than IMMPDA. As expected, these simulation results show increased difficulty for $P_d = 0.9$ when compared to $P_d = 1$ and for $\lambda = 0.001$ when compared to $\lambda = 0$. Furthermore $\lambda = 0.001$ has more impact on the performance than $P_d = 0.9$. This can be explained by the fact that for $\lambda = 0.001$ a target track may diverge because of false measurements. The SIR-H joint particle filter suffers the least from this.

Measured in terms of "both tracks OK" (Table II and figures 2a-5a) the SIR-H joint particle filter performed best, the IMMJFDA* second best, the SIR-H joint particle filter third and the IMMJFDA fourth. The both tracks "OK" figures (2a-5a) show a slight difference for $d < 0$ and $d > 0$. This is because for $d < 0$ the target trajectories cross each other before they have reached zero velocity, while for $d > 0$ they do not cross (see figure 1).

Figures 2a-5a show that IMMJFDA and IMMJFDA* filters have oscillating variation in performance which is lacking for SIR-H joint particle filter. This phenomenon can be explained by the observation that the effect of "overshoot" during a manoeuvre is for IMMJFDA and IMMJFDA* more profound than for the SIR-H joint particle filter, because the latter filters perform time extrapolation from only one state estimate per mode, whereas the SIR-H joint particle filter performs time extrapolation for many particles per mode. The effect is that for some d values IMMJFDA and IMMJFDA* actually benefit from overshoot in the sense that it keeps the tracks separated, while for other d values the overshoot actually moves the tracks closer to each other. This effect is less profound for the SIR-H joint particle filters due to time extrapolation for many particles per mode; hence oscillating variation in performance does not occur.

Rather surprisingly, IMMJFDA* outperforms Hybrid SIR joint particle filter regarding the both tracks "OK" or "swapped" criterion (Table III and figures 2b-5b) on the "easy" scenarios 1-3. Scenario 4 shows that IMMJFDA* also is outperformed on this criterion by the SIR-H joint particle filter when missing and false measurement conditions become more challenging.

Table IV and Figures 2c-5c show that IMMJFDA* performs best on track coalescence avoidance. Next best are the two particle filters, and fourth is IMMJFDA. The "dip" in "mean time in coalescence" around zero is due to the definition of "coalescing tracks". That is, when the targets are actually moving very close to each other, which is the case for small d values, there are no coalescing scans counted. Scans are only counted coalescing when the targets are separated from each other far enough.

TABLE V
AVERAGE CPU TIME PER SCAN (IN MILLISECONDS).

Sc.	IMMPDA	IMMJFDA	IMMJFDA*	SIR joint	SIR-H joint
1	16	22	23	385	439
2	38	54	48	7245	7959
3	14	20	20	377	438
4	38	61	56	7170	7810

Table V indicates a significant CPU-time increase for joint particle filters relative to the others. The increase is one order of magnitude for scenarios without clutter and two orders of magnitude for scenarios with clutter.

It should be noticed that there are various complementary methods available that allow to reduce the number of particles

and/or CPU time significantly without reducing performance (e.g. [1], [38]). Hence when reading Table V one should be aware that these methods have not been investigated in this paper.

10. CONCLUDING REMARKS

In this paper we studied the problem of maneuvering target tracking from possibly missing and false measurements. The density of the false measurements was assumed to be non-homogeneous. For this problem we studied particle filtering as an alternative for a multi-target track maintenance versions of IMM in combination with PDA or JPDA. The approach taken is to first characterize the problem in terms of filtering for a jump linear descriptor system with both Markovian and i.i.d. coefficients, and next to use this for the derivation of the exact recursive equation for the Bayesian filter (Theorem 1). This result has been used to develop two SIR type particle filters, one which resamples a fixed number of joint particles (SIR joint particle filter) and one which resamples a fixed number of joint particles per joint mode (SIR-H joint particle filter). We have also shown that application of the approximating assumptions of [18] to the exact Bayesian filter equations (Theorem 2) leads to a compact version of their IMMJPDA filter equations. For this (compact) IMMJPDA filter we also developed a track-coalescence-avoiding version (IMMJPDA*) by introduction of a particular pruning of permutation hypotheses. All our four novel filter algorithms cover the situation of non-homogeneous density of false measurements.

Through Monte Carlo simulations for a series of simple scenarios with two targets and two associated tracks these four novel filters have been compared to each other and to a filter which runs per track a single target IMMJPDA. All four clearly outperformed IMMJPDA. The particle filters used 10^4 joint particles; with this the SIR-H joint particle filter appears to approximate the Bayesian filter well, whereas the SIR joint particle filter did not. On all scenarios, IMMJPDA* performs significantly better than IMMJPDA and sometimes even remarkably close to the performance of the SIR-H joint particle filter. Apparently, the performance reduction by the IMMJPDA approximation of the exact Bayesian filter can be partly compensated by introducing the additional IMMJPDA* approximation. IMMJPDA and IMMJPDA* have in common to perform less good as the SIR-H joint PF on the following two points:

- The performance of both IMMJPDA and IMMJPDA* varies heavily with changes in the geometry of encountering target paths; this varying kind of behavior is not shown by the SIR-H joint particle filter;
- The SIR-H joint particle filter is least sensitive to divergence of track because of switching to running on false measurements; this advantage shows both when targets are clearly separated from each other and when target paths come close to each other.

Recently both [12] and [47] explored the potential effect on performance of extending IMMJPDA and IMMJPDA* to joint tracking versions, i.e. to versions where the multi-target states/modes are jointly estimated. Tugnait [47] showed

slightly improved simulation results for a particular example. In [12] we showed examples where the joint tracking versions performed better and examples where they performed worse. On average, the joint tracking versions even performed worse. In [13], [14] we showed that an appropriate pruning of permutation hypothesis also yields a track-coalescence-avoiding joint tracking version. The two weak points listed above for IMMJPDA and IMMJPDA* also apply to these joint versions.

Because the computational load of IMMJPDA* is one to two orders of magnitude lower than the computational load of the SIR-H joint particle filter is, this may be a fair reason to prefer IMMJPDA* above the SIR-H joint particle filter for particular applications. One should also be aware that the efficiency of the SIR-H joint particle filter can be significantly improved by incorporating various methods from literature (e.g. [1], [38],[42]).

In addition to the option of improving the efficiency of the SIR-H joint particle filtering, it is an option to improve the adaptation of the output equations. In this paper we considered mean and covariance of target states only, and thus averaged over the states of all particles. One alternative direction might be trying to incorporate the permutation hypothesis pruning strategy of IMMJPDA* within the output equations of the SIR-H joint particle filter. Another direction [32] is to apply clustering of particles prior to averaging.

There are several other interesting extensions possible for the jump-linear descriptor framework and the novel exact and approximate filters. For example, to incorporate the target initiation and termination approach of [39], or to incorporate unresolved measurements (e.g. [31]).

ACKNOWLEDGEMENT

The authors would like to thank the anonymous reviewers for valuable suggestions in improving the paper.

REFERENCES

- [1] M. S. Arulampam, S. Maskell, N. Gordon, J. Clapp, "A tutorial on particle filters for online nonlinear/non-Gaussian Bayesian trackers," *IEEE Tr. Signal Processing*, Vol. 50 (2002), pp. 174-188.
- [2] D. Avitzour, "Stochastic simulation Bayesian approach to multitarget tracking," *Proc. IEE Radar, Sonar and Navigation*, Vol. 142, pp. 41-44, 1995.
- [3] Y. Bar-Shalom, S. Challa, H. A. P. Blom, "IMM estimator versus optimal estimator for hybrid systems", *IEEE Trans. on Aerospace and Electronic Systems*, Vol. 41 (2005), pp. 986-991.
- [4] Y. Bar-Shalom, K.C. Chang, H.A.P. Blom, "Tracking splitting targets in clutter using an Interacting Multiple Model Joint Probabilistic Data Association filter", Ed: Y. Bar-Shalom, *Multitarget Multisensor Tracking*, Vol. II, Artech House, 1992, pp. 93-110.
- [5] Y. Bar-Shalom, R. Li, "Multitarget-multisensor tracking: Principles and techniques, 1995.
- [6] H. A. P. Blom, "An efficient filter for abruptly changing systems," *Proc. 23th IEEE Conference on Decision and Control*, (1984), pp. 656-658.
- [7] H. A. P. Blom and Y. Bar-Shalom, "The Interacting Multiple Model algorithm for systems with Markovian switching coefficients," *IEEE Tr. on Automatic Control*, Vol. 33 (1988), pp. 780-783.
- [8] H. A. P. Blom and E. A. Bloem, "Probabilistic Data Association Avoiding Track Coalescence," *IEEE Tr. on Automatic Control*, Vol. 45 (2000), pp. 247-259.
- [9] H. A. P. Blom and E. A. Bloem, "Combining IMM and JPDA for tracking multiple maneuvering targets in clutter," *Proc. 5th Int. Conf. on Information Fusion*, July 8-11, 2002, Annapolis, MD, USA, Vol. 1, pp. 705-712.

- [10] H. A. P. Blom and E. A. Bloem, "Interacting Multiple Model Joint Probabilistic Data Association avoiding track coalescence," *Proc. IEEE Conference on Decision and Control*, December 2002, pp. 3408-3415.
- [11] H. A. P. Blom and E. A. Bloem, "Joint IMM/PDA particle filter," *Proc. Fusion 2003*, Cairns, Australia, July 2003.
- [12] H. A. P. Blom and E. A. Bloem, "Tracking multiple maneuvering targets by joint combinations of IMM and PDA," *Proc. 42nd IEEE Conf. on Decision and Control*, Maui, 2003.
- [13] H. A. P. Blom, E. A. Bloem, "Joint IMM and Coupled PDA to track closely spaced targets and to avoid track coalescence," *Proc. Fusion 2004*, Stockholm, Sweden.
- [14] H. A. P. Blom, and E. A. Bloem, "Exact Bayesian filter and joint IMM coupled PDA tracking of maneuvering targets from possibly missing and false measurements," *Automatica*, Vol. 42 (2006), pp. 127-135.
- [15] Y. Boers & J. N. Driessen, "Particle filter based detection for tracking," *Proc. American Control Conf.*, June 2001, pp. 4393-4397.
- [16] Y. Boers and H. Driessen, "Hybrid state estimation: a target tracking application," *Automatica*, vol. 38 (2002) pp. 2153-2158.
- [17] Y. Boers, J. N. Driessen, F. Verschure, W. P. M. H. Heemels, A. Juloski, "A multi target track before detect application," *Proc. IEEE Conf. on Computer Vision and Pattern Recognition*, June 2003.
- [18] B. Chen and J. K. Tugnait, "Tracking of multiple maneuvering targets in clutter using IMM/JPDA filtering and fixed-lag smoothing," *Automatica*, vol. 37, pp. 239-249, Feb. 2001.
- [19] L. Dai, "Singular control systems," *Lecture notes in Control and information sciences*, Vol. 118, Springer, 1989.
- [20] M. De Feo, A. Graziano, R. Miglioli, A. Farina, "IMMJPDA versus MHT and Kalman filter with NN correlation: performance comparison", *IEE Proc. Radar, Sonar, Navigation*, Vol. 144 (1997), pp. 49-56.
- [21] A. Doucet, "On sequential simulation-based methods for Bayesian filtering." Technical Report CUED/F-INFENG/TR.310, Department of Engineering, University of Cambridge, 1998.
- [22] A. Doucet, N. J. Gordon and V. Krishnamurthy, "Particle Filters for State Estimation of Jump Markov Linear Systems," *IEEE Tr. on Signal Processing*, Vol. 49, 2001, pp. 613-624.
- [23] R. J. Elliott, F. Dufour, D. D. Sworder, "Exact hybrid filters in discrete time", *IEEE Tr. Automatic Control*, Vol. 41 (1996), pp. 1807-1810.
- [24] R. J. Fitzgerald, "Development of practical PDA logic for multitarget tracking by micro processor", Ed.: Y. Bar-Shalom, *Multitarget-Multisensor Tracking*, Artech House, 1990, pp. 1-23.
- [25] M. Gauvrit, "Bayesian adaptive filter for tracking with measurements of uncertain origin," *Automatica*, Vol. 20 (1984), pp. 217-224.
- [26] N. J. Gordon, "A hybrid bootstrap filter for target tracking in clutter," *IEEE Tr. AES*, Vol. 33 (1997), pp. 353-358.
- [27] N. Gordon, D. Salmon, D. Fisher, "Bayesian target tracking after group pattern distortion", *Proc. SPIE*, 1997, pp. 238-248.
- [28] N. J. Gordon, D. J. Salmond and A. F. M. Smith, "Novel approach to nonlinear/non-Gaussian Bayesian state estimation," *IEE Proceedings-F*, Vol. 140, pp. 107-113, 1993.
- [29] C. Hue, J. P. Le Cadre, P. Perez, "Tracking multiple objects with particle filtering," *IEEE Tr. AES*, Vol. 38 (2002), pp. 791-811.
- [30] R. Karlsson, F. Gustafsson, "Monte Carlo data association for multiple target tracking," *Proc. IEE Seminar Target Tracking: Algorithms and Applications*, October 2001, pp. 13/1-13/5.
- [31] W. Koch, G. Van Keuk, "MHT maintenance with possibly unresolved measurements," *IEEE Tr. AES*, Vol. 33 (1997), pp. 883-892.
- [32] C. Kreucher, K. Kastella, A. O. Hero, "Tracking multiple targets using a particle filter representation of the joint multitarget probability density," *Proc. SPIE Int. Symp. On Optical Science and Technology*, San Diego, August 2003.
- [33] J. MacCormick, A. Blake, "A probabilistic exclusion principle for tracking multiple objects," *Proc. 7th Int. Conf. Computer Vision*, Greece, 1999, pp. 572-580.
- [34] J. MacCormick, M. Isard, "Bramble: a Bayesian multiple-blob tracker," *Proc. 8th Int. Conf. Computer Vision*, Vancouver, July 2001, pp. 34-41.
- [35] S. Maskell, M. Rollason, N. Gordon, D. Salmond, "Efficient particle filtering for multiple target tracking with application to tracking in structured images," *Proc. Signal and Data Processing of Small Targets*, Orlando 2002, SPIE, Vol. 4728.
- [36] S. McGinnity and G. W. Irwin, "Multiple Model Bootstrap Filter for Maneuvering Target Tracking," *IEEE Tr. on Aerospace and Electronic Systems*, Vol. 36, 2000, pp. 1006-1012.
- [37] S. McGinnity and G. W. Irwin, "Maneuvering Target Tracking using a Multiple-Model Bootstrap Filter," Eds. A. Doucet, N. de Freitas and N. Gordon, *Sequential Monte Carlo Methods in Practice*, Springer 2001, pp. 479-497.
- [38] M. Morelande, S. Challa, "Maneuvering target tracking in clutter using particle filters," *IEEE Tr. AES*, Vol. 41 (2005), pp. 252-270.
- [39] D. Mušicki, R. Evans, "Clutter map information for data association and track initiation," *IEEE Tr. AES*, vol. 40 (2004), pp.387-398.
- [40] M. Orton, W. Fitzgerald, "A Bayesian approach to tracking multiple targets using sensor arrays and particle filters," *IEEE Tr. Signal Processing*, Vol. 50 (2002), pp. 216-223.
- [41] M. Orton, A. Marrs, "A Bayesian approach to multi-target tracking and data fusion with out-of-sequence measurements," *Proc. IEE Seminar Target Tracking: Algorithms and Applications*, October 2001, pp. 15/1-15/5.
- [42] B. Ristic, S. Arulampalam, N. Gordon, "Beyond the Kalman filter - Particle filters for tracking applications", Artech House, 2004.
- [43] D. B. Rubin, "Using the SIR algorithm to simulate posterior distributions," In *Bayesian Statistics*, volume 3, pages 395-402. Oxford University Press, 1988.
- [44] D. J. Salmon & H. Birch, "A particle filter for track-before-detect," *Proc. American Control Conf.*, June 2001, pp. 3755-3760.
- [45] D. J. Salmond, D. Fisher, N. J. Gordon, "Tracking and identification for closely spaced objects in clutter," *Proc. European Control Conf.*, 1997.
- [46] D. Schulz, W. Burgard, D. Fox, A. B. Cremers, "People tracking with mobile robots using sample-based Joint Probabilistic Data Association filters," *The International Journal of Robotics Research*, Vol. 22 (2003), pp. 99-116.
- [47] J. K. Tugnait, "Tracking of multiple maneuvering targets in clutter using multiple sensors, IMM and JPDA coupled filtering," *IEEE Trans. Aerospace & Electronic Systems*, Vol. 40 (2004), pp. 320-330.
- [48] J. Vermaak, S. J. Godsill, P. Perez, "Monte Carlo filtering for multi-target tracking and data association," *IEEE Tr. AES*, Vol. 41 (2005), pp. 309-331.

APPENDIX A

Proof: If $\phi = 0$ we get

$$p_{x_t|\theta_t, \phi_t, \tilde{x}_t, Y_t}(x | \theta, 0, \tilde{x}) = p_{x_t|\theta_t, Y_{t-1}}(x | \theta) \quad (\text{A.1})$$

Else, i.e. $\phi \neq 0$:

$$\begin{aligned} p_{x_t|\theta_t, \phi_t, \tilde{x}_t, Y_t}(x | \theta, \phi, \tilde{x}) &= \\ &= p_{x_t|\theta_t, \phi_t, \tilde{x}_t, y_t, L_t, Y_{t-1}}(x | \theta, \phi, \tilde{x}, y_t, L_t) = \\ &= p_{x_t|\theta_t, \phi_t, \tilde{x}_t, y_t, L_t, \tilde{y}_t, Y_{t-1}}(x | \theta, \phi, \tilde{x}, y_t, L_t, \tilde{y}_t) = \\ &= p_{x_t|\theta_t, \phi_t, \tilde{y}_t, Y_{t-1}}(x | \theta, \phi, \tilde{x}, y_t) = \\ &= p_{z_t|x_t, \theta_t, \phi_t}(\tilde{x} y_t | x, \theta, \phi) \cdot p_{x_t|\theta_t, Y_{t-1}}(x | \theta) / F_t(\phi, \tilde{x}, \theta) \end{aligned} \quad (\text{A.2})$$

with

$$F_t(\phi, \tilde{x}, \theta) \triangleq p_{z_t|\theta_t, \phi_t, Y_{t-1}}(\tilde{x} y_t | \theta, \phi) \quad (\text{A.3})$$

Subsequently

$$\begin{aligned} \beta_t(\phi, \tilde{x}, \theta) &\triangleq \text{Prob}\{\phi_t = \phi, \tilde{x}_t = \tilde{x}, \theta_t = \theta | Y_t\} = \\ &= p_{\phi_t, \tilde{x}_t, \theta_t | Y_t}(\phi, \tilde{x}, \theta) = \\ &= p_{\phi_t, \tilde{x}_t, \theta_t | y_t, L_t, Y_{t-1}}(\phi, \tilde{x}, \theta | y_t, L_t) = \\ &= p_{y_t, \tilde{x}_t, \theta_t | \phi_t, L_t, Y_{t-1}}(y_t, \tilde{x}, \theta | \phi, L_t) \cdot \\ &\quad \cdot p_{\phi_t | L_t, Y_{t-1}}(\phi | L_t) / c_t' = \\ &= p_{y_t, \tilde{x}_t | \theta_t, \phi_t, L_t, Y_{t-1}}(y_t, \tilde{x} | \theta, \phi, L_t) \cdot \\ &\quad \cdot p_{\phi_t | L_t, Y_{t-1}}(\phi | L_t) p_{\theta_t | Y_{t-1}}(\theta) / c_t' \end{aligned} \quad (\text{A.4})$$

If $\phi \neq 0$, we have $D_t > 0$ and

$$\tilde{x}_t^T \tilde{x}_t = \Phi(\psi_t)^T \chi_t \chi_t^T \Phi(\psi_t) = \Phi(\psi_t)^T \Phi(\psi_t) = \text{Diag}\{\psi_t\} \quad (\text{A.5})$$

Hence

$$\psi_t = \text{Diag}\{\psi_t\} 1_{L_t} = \tilde{x}_t^T \tilde{x}_t 1_{L_t}$$

with 1_{L_t} an L_t column vector with L_t 1-valued components. Moreover, because

$$\tilde{\chi}_t \Phi(\psi_t)^T = \chi_t^T \Phi(\psi_t) \Phi(\psi_t)^T = \chi_t^T \quad (\text{A.6})$$

this shows that the transformation from (ψ_t, χ_t) into $\tilde{\chi}_t$ has an inverse. For the first term at the right hand side of (A.4) this implies:

$$\begin{aligned} p_{y_t, \tilde{\chi}_t | \theta_t, \phi_t, L_t, Y_{t-1}}(y_t, \chi^T \Phi(\psi) | \theta, \phi, L_t) &= \\ &= p_{y_t, \psi_t, \chi_t | \theta_t, \phi_t, L_t, Y_{t-1}}(y_t, \psi, \chi | \theta, \phi, L_t) \end{aligned} \quad (\text{A.7})$$

Furthermore, because the transformation from (y_t, ψ_t, χ_t) into $(\tilde{z}_t, f_t, \psi_t, \chi_t)$ is a permutation, we get for $L_t > D(\phi) > 0$

$$\begin{aligned} p_{y_t, \psi_t, \chi_t | \theta_t, \phi_t, L_t, Y_{t-1}}(y_t, \psi, \chi | \theta, \phi, L_t) &= \\ &= p_{\tilde{z}_t, f_t, \psi_t, \chi_t | \theta_t, \phi_t, L_t, Y_{t-1}}(\chi^T \Phi(\psi) y_t, \Phi(1_{L_t} - \psi) y_t, \psi, \chi | \\ &\quad | \theta, \phi, L_t) \end{aligned} \quad (\text{A.8})$$

Substituting (A.8) in (A.7) and this in (A.4) yields:

$$\begin{aligned} \beta_t(\phi, \chi^T \Phi(\psi), \theta) &= \\ &= p_{\tilde{z}_t, f_t, \psi_t, \chi_t | \theta_t, \phi_t, L_t, Y_{t-1}}(\chi^T \Phi(\psi) y_t, \Phi(1_{L_t} - \psi) y_t, \psi, \chi | \\ &\quad | \theta, \phi, L_t) \cdot p_{\phi_t | L_t, Y_{t-1}}(\phi | L_t) p_{\theta_t | Y_{t-1}}(\theta) / c'_t \end{aligned} \quad (\text{A.9})$$

Hence, for $L_t > D(\phi) > 0$, this yields:

$$\begin{aligned} \beta_t(\phi, \chi^T \Phi(\psi), \theta) &= p_{\tilde{z}_t | \theta_t, \phi_t, Y_{t-1}}(\chi^T \Phi(\psi) y_t | \theta, \phi) \cdot \\ &\cdot p_{f_t | \phi_t, \psi_t, L_t}(\Phi(1_{L_t} - \psi) y_t | \phi, \psi) p_{\psi_t | \phi_t, L_t}(\psi | \phi) \cdot \\ &\cdot p_{\chi_t | \phi_t}(\chi | \phi) p_{L_t | \phi_t}(L_t | \phi) p_{\phi_t}(\phi) p_{\theta_t | Y_{t-1}}(\theta) / c'' \end{aligned} \quad (\text{A.10})$$

Evaluation of the terms in (A.10) yields:

$$\begin{aligned} p_{f_t | \phi_t, \psi_t, L_t}(\Phi(1_{L_t} - \psi) y_t | \phi, \psi) &= \\ &= p_{f_t | F_t, \psi_t}(\Phi(1_{L_t} - \psi) y_t | L_t - D(\phi), \psi) = \\ &\stackrel{(6.b)}{=} \prod_{i=1}^{L_t - D(\phi)} p_f([\Phi(1_{L_t} - \psi) y_t]_i) = \\ &= \prod_{i=1}^{L_t - D(\phi)} p_f([\Phi(1_{L_t} - \tilde{\chi}^T \tilde{\chi} 1_{L_t}) y_t]_i) \end{aligned} \quad (\text{A.11})$$

$$p_{\psi_t | \phi_t, L_t}(\psi | \phi, L_t) = D(\phi)! (L_t - D(\phi))! / L_t! \quad (\text{A.12})$$

$$p_{\chi_t | \phi_t}(\chi | \phi) = 1 / D(\phi)! \quad (\text{A.13})$$

$$\begin{aligned} p_{L_t | \phi_t}(L_t | \phi) &= p_{F_t}(L_t - D(\phi)) = \\ &= (\hat{F}_t)^{(L_t - D(\phi))} \exp\{-\hat{F}_t\} / (L_t - D(\phi))! \\ &\quad \text{if } L_t \geq D(\phi) \\ &= 0 \quad \text{if } L_t < D(\phi) \end{aligned} \quad (\text{A.14})$$

$$p_{\phi_t}(\phi) = \prod_{i=1}^M [(P_d^i)^{\phi_i} (1 - P_d^i)^{1 - \phi_i}] \quad (\text{A.15})$$

Substituting (A.3) and (A.11) through (A.15) into (A.10) and subsequent evaluation yields for $L_t > D(\phi) > 0$:

$$\begin{aligned} \beta_t(\phi, \chi^T \Phi(\psi), \theta) &= F_t(\phi, \chi^T \Phi(\psi), \theta) \cdot \\ &\cdot \hat{F}_t^{(L_t - D(\phi))} \cdot \prod_{j=1}^{L_t - D(\phi)} p_f([\Phi(1_{L_t} - \tilde{\chi}^T \tilde{\chi} 1_{L_t}) y_t]_j) \cdot \\ &\cdot \prod_{i=1}^M [(P_d^i)^{\phi_i} (1 - P_d^i)^{1 - \phi_i}] \cdot p_{\theta_t | Y_{t-1}}(\theta) / c_t \end{aligned}$$

with c_t a normalizing constant. It can be easily verified that the last equation also holds true if $L_t = D(\phi)$ or if $D(\phi) = 0$. Together with (6.c) this yields (14). \blacksquare

APPENDIX B

Proof: From the proof of Proposition 1 we have

$$\begin{aligned} F_t(\phi, \tilde{\chi}, \theta) &= p_{\tilde{z}_t | \theta_t, \phi_t}(\tilde{\chi} y_t | \theta, \phi) = \\ &= \int_{\mathbb{R}^{Mn}} p_{\tilde{z}_t | x_t, \theta_t, \phi_t, Y_{t-1}}(\tilde{\chi} y_t | x, \theta, \phi) \cdot \\ &\quad \cdot p_{x_t | \theta_t, \phi_t, Y_{t-1}}(x, \theta) dx \end{aligned} \quad (\text{B.1})$$

$$\begin{aligned} p_{\tilde{z}_t | x_t, \theta_t, \phi_t}(\tilde{\chi} y_t | x, \theta, \phi) &= \\ &= \prod_{\substack{i=1 \\ \phi^i=1}}^M p_{\tilde{z}_t^i | x_t^i, \theta_t^i}([\Phi(\phi) \tilde{\chi}]_{ik} y_t^k | x^i, \theta^i) \end{aligned} \quad (\text{B.2})$$

This together with C2) yields:

$$F_t(\phi, \tilde{\chi}, \theta) = \prod_{i=1}^M f_t^i(\phi, \tilde{\chi}, \theta) \quad (\text{B.3})$$

with

$$\begin{aligned} f_t^i(\phi, \tilde{\chi}, \theta) &= \int_{\mathbb{R}^n} p_{\tilde{z}_t^i | x_t^i, \theta_t^i}([\Phi(\phi) \tilde{\chi}]_{ik} y_t^k | x^i, \theta^i) \cdot \\ &\quad \cdot p_{x_t^i | \theta_t^i, Y_{t-1}}(x^i | \theta^i) dx^i \quad \text{if } \phi^i = 1 \\ &= 1 \quad \text{if } \phi^i = 0 \end{aligned} \quad (\text{B.4})$$

Together with C3) the last two equations yield (29) and (30.a,b,c).

Substitution of (B.2) and C2) into (13) yields

$$\begin{aligned} p_{x_t^i | \theta_t^i, \phi_t^i, \tilde{\chi}_t, Y_t}(x^i | \theta^i, \phi, \tilde{\chi}) &= \\ &= \frac{p_{\tilde{z}_t^i | x_t^i, \theta_t^i}([\Phi(\phi) \tilde{\chi}]_{ik} y_t^k | x^i, \theta^i) \cdot p_{x_t^i | \theta_t^i, Y_{t-1}}(x^i | \theta^i)}{f_t^i(\phi, \tilde{\chi}, \theta)} \end{aligned} \quad (\text{B.5})$$

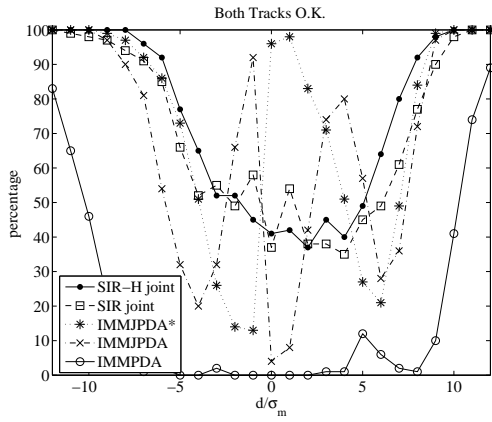
If $p_{x_t^i | \theta_t^i, Y_{t-1}}(x^i | \theta^i)$ is Gaussian with mean $\bar{x}_t^i(\theta^i)$ and covariance $\bar{P}_t^i(\theta^i)$, then the density $p_{x_t^i | \phi_t^i, \tilde{\chi}_t, \theta_t^i, Y_t}(x^i | \phi, \tilde{\chi}, \theta^i)$ is Gaussian with mean $\hat{x}_t^i(\phi, \tilde{\chi}, \theta^i)$ and covariance $\hat{P}_t^i(\phi, \theta^i)$ satisfying for $\phi^i \neq 0$,

$$\begin{aligned} \hat{x}_t^i(\phi, \tilde{\chi}, \theta^i) &= \bar{x}_t^i(\theta^i) + K_t^i(\phi, \theta^i) [[\tilde{\chi} y_t]_i - h^i(\theta^i) \bar{x}_t^i(\theta^i)] \\ \hat{P}_t^i(\phi, \theta^i) &= \bar{P}_t^i(\theta^i) - K_t^i(\phi, \theta^i) h^i(\theta^i) \bar{P}_t^i(\theta^i) \end{aligned}$$

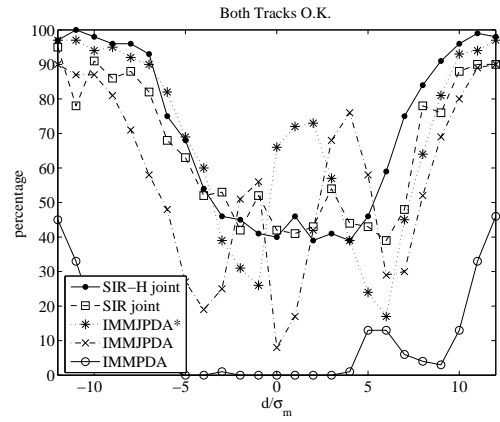
and for $\phi^i = 0$:

$$\begin{aligned} \hat{x}_t^i(\phi, \tilde{\chi}, \theta^i) &= \bar{x}_t^i(\theta^i) \\ \hat{P}_t^i(\phi, \theta^i) &= \bar{P}_t^i(\theta^i) \end{aligned}$$

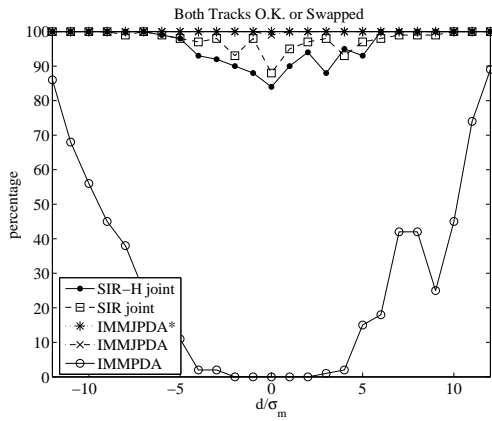
Hence, $p_{x_t^i | \theta_t^i, Y_t}(\cdot | \theta^i)$ is a Gaussian mixture, and all equations in Theorem 2 follow from a lengthy but straightforward evaluation of this mixture. \blacksquare



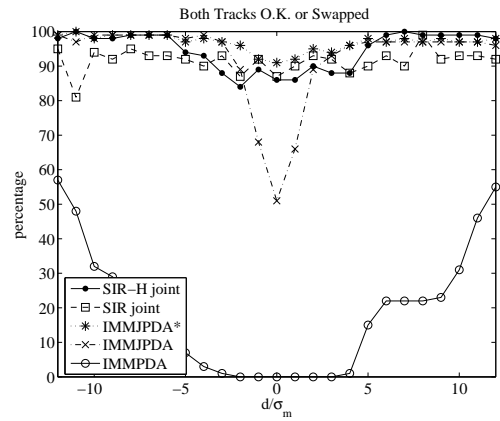
2a. Both tracks "OK" percentage



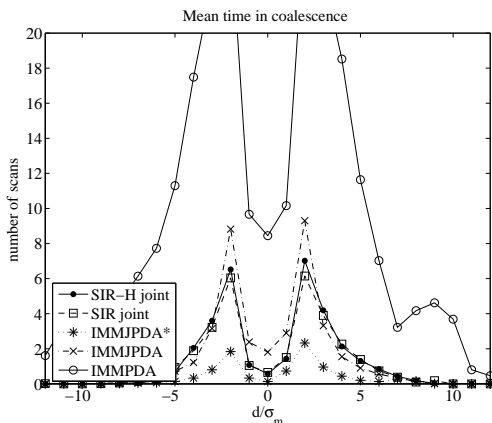
3a. Both tracks "OK" percentage



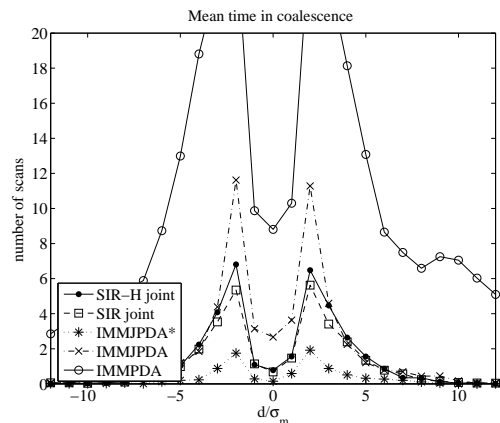
2b. Both tracks "OK" or "Swapped" percentage



3b. Both tracks "OK" or "Swapped" percentage



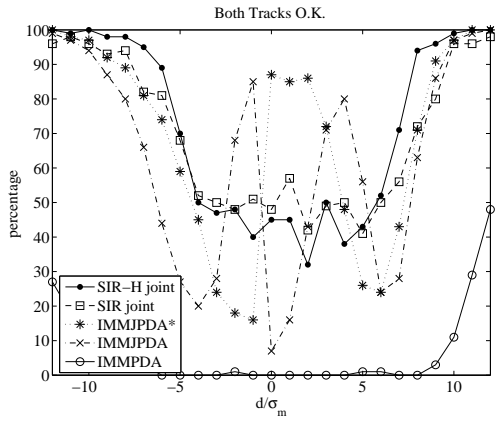
2c. Average number of "coalescing" scans



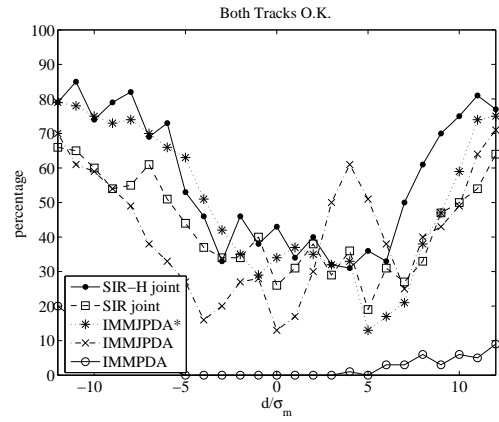
3c. Average number of "coalescing" scans

Fig. 2. Simulation results for scenario 1

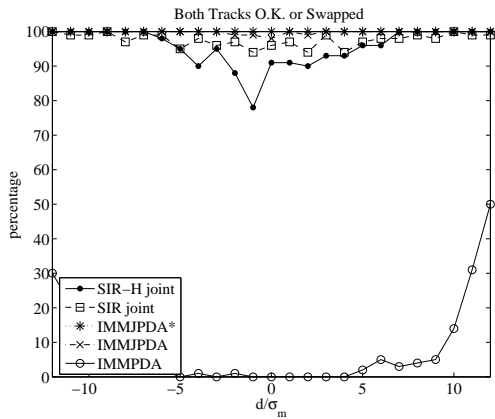
Fig. 3. Simulation results for scenario 2



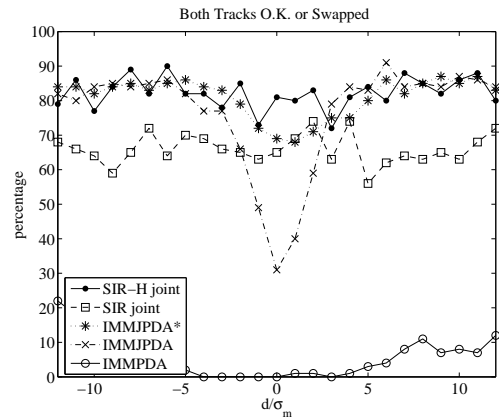
4a. Both tracks "OK" percentage



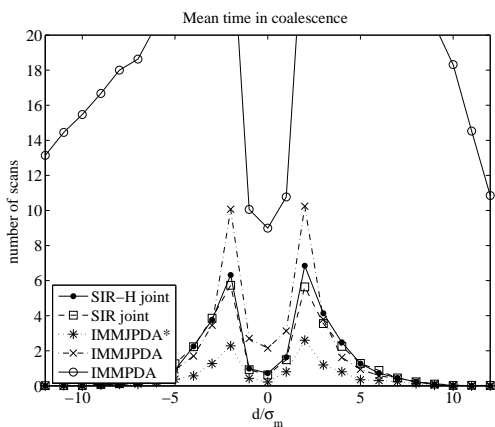
5a. Both tracks "OK" percentage



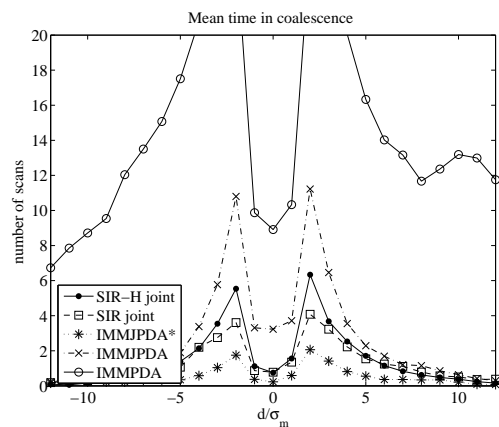
4b. Both tracks "OK" or "Swapped" percentage



5b. Both tracks "OK" or "Swapped" percentage



4c. Average number of "coalescing" scans



5c. Average number of "coalescing" scans

Fig. 4. Simulation results for scenario 3

Fig. 5. Simulation results for scenario 4